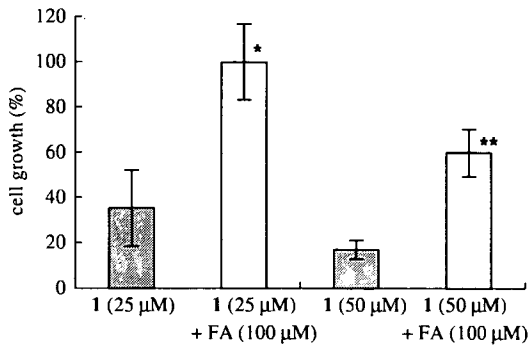

Figure 4. Growth inhibition of FR-positive MCF-7 cells by **1** and **1** plus 100 μM free folic acid (FA). $^{*}p < 0.05$; $^{**}p < 0.01$ by Student's *t* test.

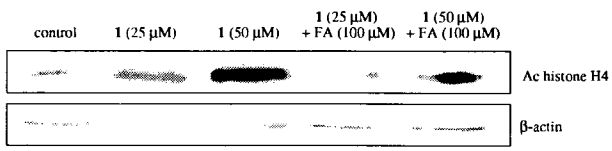

Figure 5. Western blot analysis of histone hyperacetylation in MCF-7 cells produced by **1** and **1** plus 100 μM free folic acid (FA).

a disulfide bond to connect a thiolate HDAC inhibitor with folic acid should be applicable to other anticancer agents bearing a thiol group, such as thiolate matrix metalloproteinase inhibitors[27] and thiolate farnesyltransferase inhibitors.[28] Our findings in this study provide the basis for a new approach to developing candidate antitumor agents with potentially fewer side effects.

Acknowledgments

This work was supported in part by Grants-in-Aid for Young Scientists (B) from the Ministry of Education, Science, Culture, Sports, Science, and Technology, Japan, and a grant from Takeda Science Foundation.

References and notes

1. Miller, T. A.; Witter, D. J.; Belvedere, S. *J. Med. Chem.* **2003**, *46*, 5097.
2. Miller, T. A. *Expert Opin. Ther. Pat.* **2004**, *14*, 791.
3. Biel, M.; Wascholowski, V.; Giannis, A. *Angew. Chem. Int. Ed. Engl.* **2005**, *44*, 3186.
4. Suzuki, T.; Miyata, N. *Curr. Med. Chem.* **2006**, *13*, 935.
5. Richon, V. M.; Emiliani, S.; Verdin, E.; Webb, Y.; Breslow, R.; Rifkind, R. A.; Marks, P. A. *Proc. Natl. Acad. Sci. U.S.A.* **1998**, *95*, 3003.
6. Saito, A.; Yamashita, T.; Mariko, Y.; Nosaka, Y.; Tsuchiya, K.; Ando, T.; Suzuki, T.; Tsuruno, T.; Nakanishi, O. *Proc. Natl. Acad. Sci. U.S.A.* **1999**, *96*, 4592.
7. Kelly, W. K.; Richon, V. M.; O'Connor, O.; Curley, T.; MacGregor-Curtelli, B.; Tong, W.; Klang, M.; Schwartz, L.; Richardson, S.; Rosa, E.; Drobnjak, M.; Cordon-Cordo, C.; Chiao, J. H.; Rifkind, R.; Marks, P. A.; Scher, H. *Clin. Cancer Res.* **2003**, *9*, 3578.
8. Kelly, W. K.; O'Connor, O. A.; Krug, L. M.; Chiao, J. H.; Heaney, M.; Curley, T.; MacGregore-Cortelli, B.; Tong, W.; Secrist, J. P.; Schwartz, L.; Richardson, S.; Chu, E.; Olgac, S.; Marks, P. A.; Scher, H.; Richon, V. M. *J. Clin. Oncol.* **2005**, *23*, 3923.
9. Ryan, Q. C.; Headlee, D.; Acharya, M.; Sparreboom, A.; Trepel, J. B.; Ye, J.; Figg, W. D.; Hwang, K.; Chung, E. J.; Murgo, A.; Melillo, G.; Elsayed, Y.; Monga, M.; Kalnitskiy, M.; Zwiebel, J.; Sausville, E. A. *J. Clin. Oncol.* **2005**, *23*, 3912.
10. Antony, A. C. *Blood* **1992**, *79*, 2807.
11. Ross, J. F.; Chaudhuri, P. K.; Ratnam, M. *Cancer* **1994**. *73*, 2432.
12. Weitman, S. D.; Lark, R. H.; Coney, L. R.; Fort, D. W.; Frasca, V.; Zurawski, V. R.; Kamen, B. A. *Cancer Res.* **1992**, *52*, 3396.
13. Weitman, S. D.; Weinberg, A. G.; Coney, L. R.; Zurawski, V. R.; Jennings, D. S.; Kamen, B. A. *Cancer Res.* **1992**, *52*, 6708.
14. Leamon, C. P.; Reddy, J. A. *Adv. Drug Deliv. Rev.* **2004**, *56*, 1143.
15. Canevari, S.; Mezzanzanica, D.; Menard, S.; Ferrini, S.; Moretta, L.; Colnaghi, M. I. *Int. J. Cancer* **1992**, *7*, 42.
16. Yamaguchi, T.; Tsurumi, H.; Kotani, T.; Yamaoka, N.; Otsuji, E.; Kitamura, K.; Takahashi, T. *Jpn. J. Cancer Res.* **1994**, *85*, 167.
17. Suzuki, T.; Kouketsu, A.; Matsuura, A.; Kohara, A.; Ninomiya, S.; Kohda, K.; Miyata, N. *Bioorg. Med. Chem. Lett.* **2004**, *14*, 3313.
18. Suzuki, T.; Matsuura, A.; Kouketsu, A.; Nakagawa, H.; Miyata, N. *Bioorg. Med. Chem. Lett.* **2005**, *15*, 331.
19. Suzuki, T.; Kouketsu, A.; Itoh, Y.; Hisakawa, S.; Maeda, S.; Yoshida, M.; Nakagawa, H.; Miyata, N. *J. Med. Chem.* **2006**, *49*, 4809.
20. Suzuki, T.; Nagano, Y.; Kouketsu, A.; Matsuura, A.; Maruyama, S.; Kurotaki, M.; Nakagawa, H.; Miyata, N. *J. Med. Chem.* **2005**, *48*, 1019.
21. Suzuki, T.; Hisakawa, S.; Itoh, Y.; Maruyama, S.; Kurotaki, M.; Nakagawa, H.; Miyata, N. *Bioorg. Med. Chem. Lett.* **2007**, *17*, 1558.
22. Luo, J.; Smith, M. D.; Lantrip, D. A.; Wang, S.; Fuchs, P. L. *J. Am. Chem. Soc.* **1997**, *119*, 10004.
23. The HDAC activity assay was performed using an HDAC fluorescent activity assay/drug discovery kit (AK-500, BIOMOL Research Laboratories). HeLa Nuclear Extracts (0.5 μL/well) were incubated at 37 °C with 25 μM of Fluor de Lys™ substrate and various concentrations of samples. Reactions were stopped after 30 min by adding Fluor de Lys™ Developer with trichostatin A which stops further deacetylation. Then, 15 min after addition of this developer, the fluorescence of the wells was measured on a fluorometric reader with excitation set at 360 nm and emission detection set at 460 nm, and the % inhibition was calculated from the fluorescence readings of inhibited wells relative to those of control wells. The concentration of compound which results in 50% inhibition was determined by plotting the log[Inh] versus the logit function of the % inhibition. IC_{50} values are determined using a regression analysis of the concentration/inhibition data.
24. MCF-7 human breast cancer cells were purchased from American Type Culture Collection (ATCC, Manassas, VA, USA) and cultured in Dulbecco's modified Eagle's medium (DMEM) containing penicillin and streptomycin, which was supplemented with fetal bovine serum as described in the ATCC instructions. MCF-7 cells were plated in 96-well plates at initial densities of 5000 cells/well (50 μL/well) and incubated at 37 °C. After 24 h, cells were exposed to a solution of test compounds in DMEM (50 μL) at various concentrations in DMEM at 37 °C in

5% CO_2 for 72 h. Then, 10 μL of alamarBlue™ was added, and cells were incubated at 37 °C for 3 h. The fluorescence of the wells was measured on a fluorometric reader with excitation set at 530 nm and emission detection set at 590 nm, and the percentage of cell growth was calculated from the fluorescence readings.

25. Lee, E. S.; Na, K.; Bae, Y. H. *J. Control. Release* **2003**, *91*, 103.
26. MCF-7 cells were cultured in DME culture medium containing penicillin and streptomycin, which was supplemented with fetal bovine serum as described in the ATCC instructions. MCF-7 cells (5×10^5) were treated for 14 h with samples at the indicated concentrations in 10% FBS-supplemented DMEM then collected and extracted with SDS buffer. Protein concentrations of the lysates were determined using a Bradford protein assay kit (Bio-Rad Laboratories); equivalent amounts of proteins from each lysate were resolved in 15% SDS–polyacrylamide gel and then transferred onto nitrocellulose membranes (Bio-Rad Laboratories). After blocking for 30 min with Tris-buffered saline (TBS) containing 3% skim milk, the transblotted membrane was incubated overnight at 4 °C with hyperacetylated histone H4 antibody (Upstate Biotechnology) (1:2000 dilution) or β-actin antibody (Abcam) (1:1000 dilution) in TBS containing 3% skim milk. After probing with the primary antibody, the membrane was washed twice with water, then incubated with goat anti-rabbit or anti-mouse IgG-horseradish peroxidase conjugates (diluted 1:5000) for 2 h at room temperature, and further washed twice with water. The immunoblots were visualized by enhanced chemiluminescence.
27. Whittaker, M.; Floyd, C. D.; Brown, P.; Gearing, A. J. H. *Chem. Rev.* **1999**, *99*, 2735.
28. Bell, I. M. *J. Med. Chem.* **2004**, *47*, 1869.

Available online at www.sciencedirect.com
ScienceDirect
Bioorganic & Medicinal Chemistry Letters 17 (2007) 4351–4357
Bioorganic & Medicinal Chemistry Letters

Phenylpropanoic acid derivatives bearing a benzothiazole ring as PPARδ-selective agonists

Hiroki Fujieda,[a] Shinya Usui,[a] Takayoshi Suzuki,[a] Hidehiko Nakagawa,[a] Michitaka Ogura,[b] Makoto Makishima[b] and Naoki Miyata[a,*]

[a]*Graduate School of Pharmaceutical Sciences, Nagoya City University, 3-1 Tanabe-dori, Mizuho-ku, Nagoya, Aichi 467-8603, Japan*
[b]*Nihon University School of Medicine, 30-1 Oyaguchi-kamicho, Itabashi-ku, Tokyo 173-8610, Japan*

Received 17 March 2007; revised 2 May 2007; accepted 8 May 2007
Available online 13 May 2007

Abstract—To find novel PPARδ-selective agonists, we designed and synthesized phenylpropanoic acid derivatives bearing 6-substituted benzothiazoles. Optimization of this series led to the identification of a potent and selective PPARδ agonist **17**. Molecular modeling suggested that compound **17** occupies the Y-shaped pocket of PPARδ appropriately.
© 2007 Elsevier Ltd. All rights reserved.

Peroxisome proliferator-activated receptors (PPARs) are members of the nuclear receptor superfamily and the PPAR subfamily consists of three members, PPARα, PPARγ, and PPARδ.[1] Many studies on PPARα and PPARγ have been performed and their roles are well established.[2,3] Further, these efforts led to the discovery of hypolipidemic agents[4] and insulin sensitizers.[5,6] Meanwhile, the role of PPARδ is just beginning to emerge. Several studies have suggested that PPARδ plays an important role in regulating lipid metabolism and energy homeostasis in muscle and adipose tissues[7–12] and the activation of PPARδ increases HDL levels, attenuates weight gain, and improves insulin sensitivity.[7,10] Thus, PPARδ-selective agonists are of interest not only as tools for elucidating the more intricate biological functions of PPARδ but also as candidate drugs for metabolic syndrome.

We previously reported compound **1** as a potent PPARγ ligand[13] and compound **2** as a potent PPARα ligand[14,15] (Fig. 1). In the course of our SAR studies on phenylpropanoic acid derivatives, we discovered that compound **4**, in which the pyridine ring of **1** is replaced by a benzothiazole ring, showed selective PPARδ activity as compared with the other aromatic compounds **1**, **3**, and **5**,[15] although the activity was not so strong (Fig. 2). Since PPARδ agonists having a benzothiazole ring have never been reported, we chose compound **4** as the lead compound for the exploration of novel PPARδ-selective agonists. We describe here the design, synthesis, and PPARδ selectivity of a series of phenylpropanoic acid derivatives bearing a 6-substituted benzothiazole ring.

The routes used for the synthesis of compounds **4**–**17** are illustrated in Schemes 1–5.

Preparation of compounds **3** and **4** is shown in Scheme 1. Ethyleneglycol **18** was allowed to react with *tert*-butyldimethylsilylchloride to give mono-alcohol **19**. Secondary amine **23**, the key intermediate for the preparation of **3** and **4**, was synthesized using a 2-nitrobenzenesulfonyl (nosyl) group[16,17]: *n*-Nonylamine **20** was treated with 2-nitrobenzenesulfonylchloride to afford *N*-nosyl nonylamine **21**. Mitsunobu reaction was applied to the conversion of **21** into *N*-alkyl compound **22**.[18] The nosyl group was removed by treating with benzenethiol in the presence of K_2CO_3 in anhydrous DMF to give a secondary amine **23**. Preparation of *N*-phenyloxazolyl compound **25a** and *N*-phenylthiazolyl compound **25b** was achieved by the method of Buchwald[19]: treatment of **23** with 2-chlorobenzoxazole or 2-chlorobenzothiazole **24**, $Pd_2(DBA)_3$, BINAP, and *tert*-BuONa in toluene. The TBS group of **25a** and **25b** was removed by treating with tetrabutylammonium fluoride (TBAF) in THF to give alcohols **26a** and **26b**,

Keywords: PPARδ; Agonist; Drug design; Nuclear receptor; Metabolic syndrome.
* Corresponding author. Tel.: +81 52 836 3407; fax: +81 52 836 3407; e-mail: miyata-n@phar.nagoya-cu.ac.jp

0960-894X/$ - see front matter © 2007 Elsevier Ltd. All rights reserved.
doi:10.1016/j.bmcl.2007.05.017

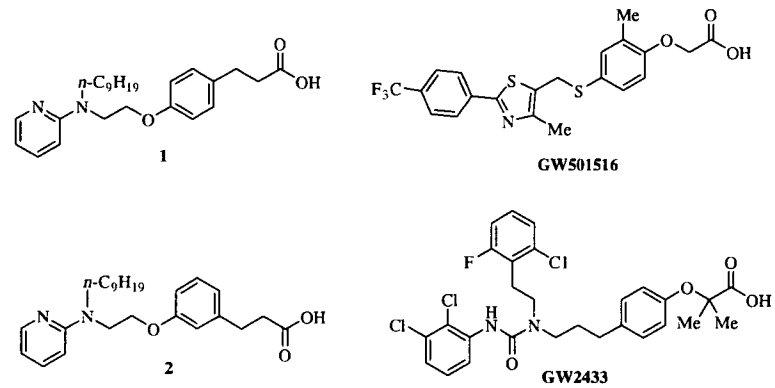

Figure 1. Structures of compounds **1** and **2**, GW501516, and GW2433.

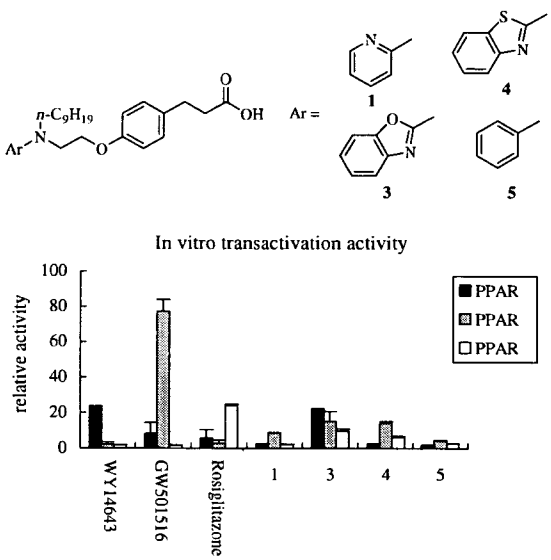

Figure 2. In vitro functional PPAR transactivation activity of compounds **1** and **3–5**. WY14643 (PPARα agonist) and GW501516 (PPARδ agonist), Rosiglitazone (PPARγ agonist) were used as reference compounds. GW501516 was used at 1 μM and others at 10 μM.

which were converted into ethers **27a** and **27b** by Mitsunobu reaction. Treatment of **27a** and **27b** with aqueous NaOH gave the desired carboxylic acids **3** and **4**.

The preparation of compound **5** is outlined in Scheme 2. *N*-phenylaminoethanol **28** was allowed to react with 1-iodononane to give *N*-alkyl compound **29**. Nucleophilic aromatic substitution by treatment of **29** with 4-fluorobenzaldehyde in the presence of sodium hydride gave ether **30**. Conversion of aldehyde **30** into **31** was achieved by Horner–Wadsworth–Emmons reaction.[20] The double bond of **31** was hydrogenated and subsequent hydrolysis gave carboxylic acid **5**.

Preparation of compounds **6**, **12**, **13**, **15**, and **16** is shown in Scheme 3. 4-Bromo-3-ethylphenol **33** was allowed to react with KI, KIO_3, and HCl to give 4-iodo-3-ethylphenol **34**.[21] The Heck reaction was applied to the conversion of **34** into **35**, and **36** into **37**.[22] Compounds **24**, **39a**, and **39b** were allowed to react with *N*-benzylaminoethanol to give tertiary amines **40a–c**. The conversion of **40a–c** into **41a–e** was achieved by Mitsunobu reaction, and subsequent hydrolysis or treatment with TFA afforded carboxylic acids **6**, **12**, **13**, **15**, and **16**.

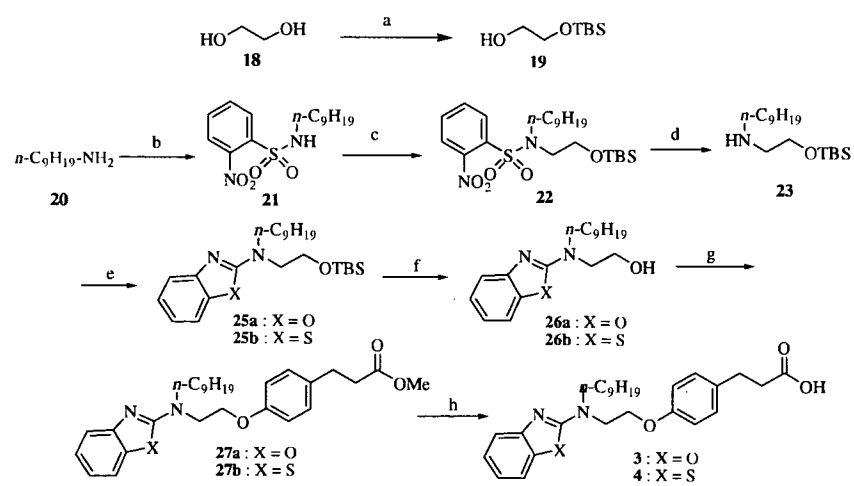

Scheme 1. Reagents and conditions: (a) *tert*-butyldimethylsilyl chloride, Et_3N, CH_2Cl_2, DMAP, rt, 75%; (b) 2-nitrobenzenesulfonyl chloride, K_2CO_3, CH_2Cl_2, rt, 93%; (c) **19**, DEAD, PPh_3, anhydrous THF, 0 °C to rt; (d) benzenethiol, K_2CO_3, anhydrous DMF, rt, 83% (2 steps); (e) 2-chlorobenzoxazole or 2-chlorobenzothiazole (**24**), $Pd_2(DBA)_3$, rac-BINAP, *tert*-BuONa, anhydrous toluene, 105 °C; (f) TBAF, THF, rt, 62–67% (2 steps); (g) methyl 3-(4-hydroxyphenyl)propionate, DEAD, PPh_3, anhydrous THF, 0 °C to rt, 70–72%; (h) 2 N aq NaOH, MeOH, THF, rt, 99–100%.

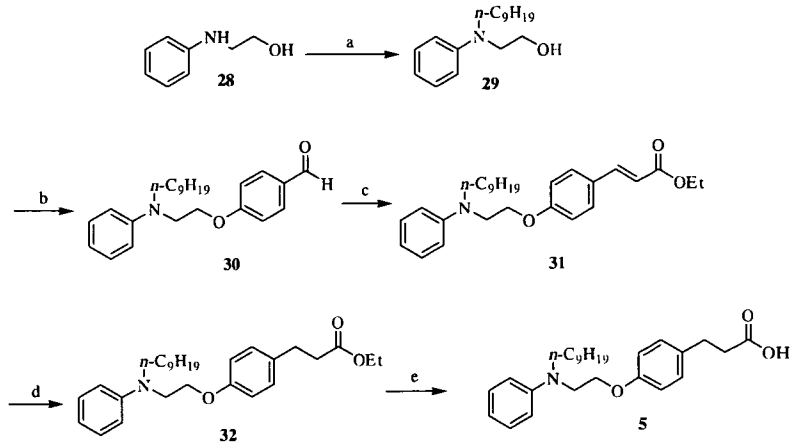

Scheme 2. Reagents and conditions: (a) 1-iodononane, 1,4-dioxane, 100 °C, 81%; (b) i—NaH, anhydrous DMF, 0 °C to 50 °C, ii—4-fluorobenzaldehyde, anhydrous DMF, rt, 26%; (c) $(EtO)_2P(O)CH_2CO_2Et$, NaH, anhydrous THF, 0 °C to rt, 42%; (d) H_2, Pd/C, MeOH, rt, 79%; (e) 2 N aq NaOH, EtOH–THF, rt, 97%.

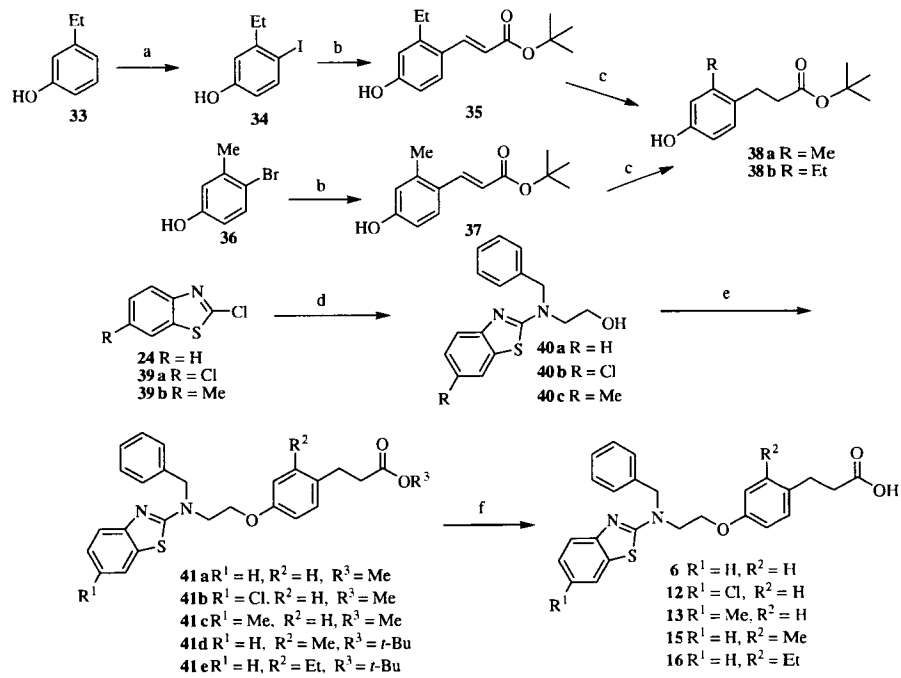

Scheme 3. Reagents and conditions: (a) KI, KIO_3, HCl, 60%; (b) *tert*-butylacrylate, $Pd(OAc)_2$, P(*o*-tol)$_3$, Et_3N, 110 °C, 58–83%; (c) H_2, Pd/C, MeOH, rt, 75–81%; (d) *N*-benzylaminoethanol, $Pd_2(DBA)_3$, rac-BINAP, *tert*-BuONa, anhydrous toluene, 80 °C or *N*-benzylaminoethanol, Et_3N, 100 °C, 44–79%; (e) methyl 3-(4-hydroxyphenyl)propionate or **38a** or **38b**, DEAD, PPh_3, anhydrous THF, 0 °C to rt, 24–77%; (f) 2 N aq NaOH, EtOH, THF, rt or TFA, CH_2Cl_2, rt, 22–81%.

Compounds **7–11** and **14** were prepared as shown in Scheme 4. Coupling between glycolic acid and amines **42a**, **42b**, and **43** afforded amides **44a**, **44b**, and **45**. Amides **44a**, **44b**, and **45** were reduced by $LiAlH_4$ to give secondary amines **46a**, **46b**, and **47**. Reductive aminoalkylation of 2-aminoethanol or 3-amino-1-propanol with **48–50** gave secondary amines **51**, **52**, and **53**. Amines **46a**, **46b**, **47**, and **51–53** were allowed to react with 2-chlorobenzothiazole **24** to give tertiary amines **54a–f**. Alcohols **54a–f** were converted into **7–11** and **14** in the same way as described for the synthesis of **3** and **4**.

Preparation of compound **17** is shown in Scheme 5. Reductive aminoalkylation of 3-amino-1-propanol with aldehyde **49** gave **56**. Amine **56** was converted to compound **17** by the same method described for the preparation of **15** and **16**.

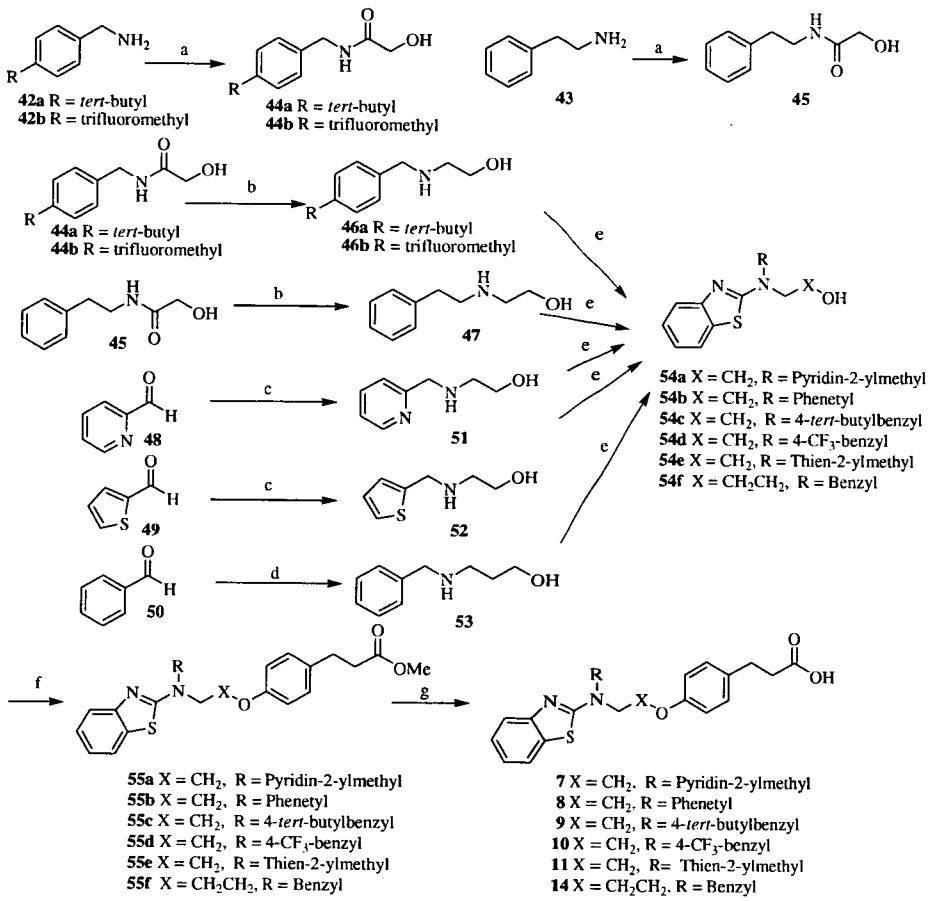

Scheme 4. Reagents and conditions: (a) glycolic acid, EDCI, DMAP, THF, rt, 51–73%; (b) $LiAlH_4$, anhydrous THF, 0 °C to reflux; (c) 2-aminoethanol, anhydrous MeOH, 0 °C, $NaBH_4$; (d) 1-amino-3-propanol, anhydrous MeOH, 0 °C, $NaBH_4$; (e) 2-chlorobenzothiazole, Et_3N, 100 °C, 10–30% (2 steps); (f) methyl 3-(4-hydroxyphenyl)propionate, DEAD, PPh_3, anhydrous THF, 0 °C to rt, 36–96%; (g) 2 N aq NaOH, EtOH, THF, rt, 15–80%.

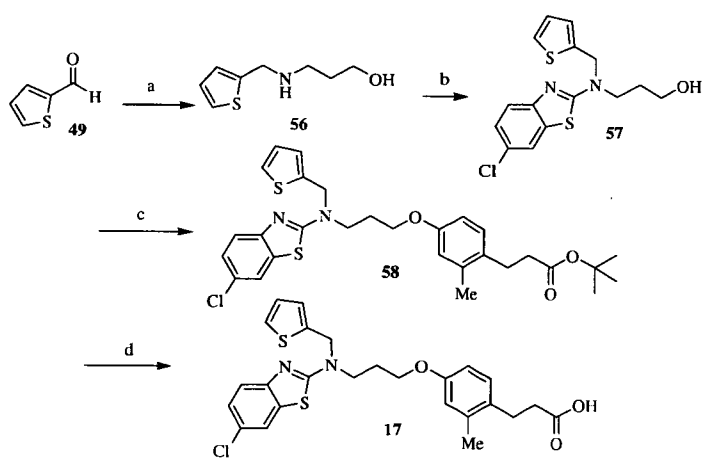

Scheme 5. Reagents and conditions: (a) 3-amino-1-propanol, MeOH, $NaBH_4$; (b) 2,6-dichlorobenzothiazole, Et_3N, 100 °C, 83% (2 steps); (c) **38a**, DEAD, PPh_3, anhydrous THF, 0 °C to rt, 64%; (d) TFA, CH_2Cl_2, rt, 73%.

Compounds **6–17** were tested in an in vitro transactivation assay against human PPAR subtypes and the results are listed in Table 1[23,24]. GW501516 (Fig. 1) was used as a reference compound.

In previous reports, the co-crystal structure of PPARδ with pan-agonist GW2433 (Fig. 1) has revealed that PPARδ has a unique Y-shaped pocket and GW2433 fills all three legs of the pocket.[25,26] The crystal structure also

Table 1. In vitro functional PPAR transactivation activity of compounds **4** and **6–17**

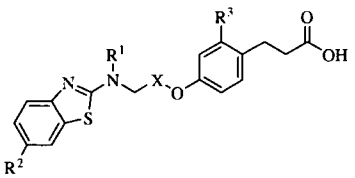

Compound	X	R^1	R^2	R^3	EC_{50}[a]		
					α (μM)	δ (μM)	γ (μM)
4	CH_2	*n*-C_9H_{19}	H	H	N.E.[b]	N.E.[b]	N.E.[b]
6	CH_2	Benzyl	H	H	N.E.[b]	2.81	N.E.[b]
7	CH_2	Pyridin-2-ylmethyl	H	H	N.E.[b]	N.E.[b]	N.E.[b]
8	CH_2	Phenethyl	H	H	N.E.[b]	N.E.[b]	N.E.[b]
9	CH_2	4-*tert*-Butylbenzyl	H	H	N.E.[b]	4.88	6.34
10	CH_2	4-CF_3-benzyl	H	H	4.46	0.94	3.69
11	CH_2	Thien-2-ylmethyl	H	H	N.E.[b]	1.74	N.E.[b]
12	CH_2	Benzyl	Cl	H	N.E.[b]	1.36	N.E.[b]
13	CH_2	Benzyl	Me	H	N.E.[b]	2.61	N.E.[b]
14	CH_2CH_2	Benzyl	H	H	N.E.[b]	2.55	N.E.[b]
15	CH_2	Benzyl	H	Me	N.E.[b]	1.17	N.E.[b]
16	CH_2	Benzyl	H	Et	N.E.[b]	2.97	N.E.[b]
17	CH_2CH_2	Thien-2-ylmethyl	Cl	Me	N.E.[b]	0.39	N.E.[b]
GW501516					N.E.[c]	0.085	N.E.[c]

[a] Compounds were screened for agonist activity on PPAR-GAL4 chimeric receptors in transiently transfected HEK-293 cells as described. EC_{50} value is the molar concentration of the test compound that affords 50% of maximal reporter activity.
[b] N.E., did not have sufficient activity to determine EC_{50} values up to 20 μM.
[c] N.E., did not have sufficient activity to determine EC_{50} values up to 10 μM.

made it clear that the two legs of the Y-shaped pocket are formed by hydrophobic amino acid residues and are not so large when compared with the hydrophobic regions of PPARα and PPARγ where the nonyl groups of compound **1** or compound **2** are estimated to be located.[13,14] Based on these information, compounds **6–11** in which the nonyl group of **4** is replaced by smaller lipophilic groups were designed and synthesized. Since compounds **6–11** could possibly have Y-shaped conformation and lack a long alkylchain which is needed for affinity to PPARα or PPARγ,[13,14] they were expected to bind PPARδ selectively. As shown in Table 1, compound **6** (R^1 = Bn), compound **9** (R^1 = 4-*tert*-butylbenzyl), compound **10** (R^1 = 4-CF_3-benzyl), and compound **11** (R^1 = thien-2-ylmethyl) were found to be PPARδ agonists more potent than lead compound **4**,

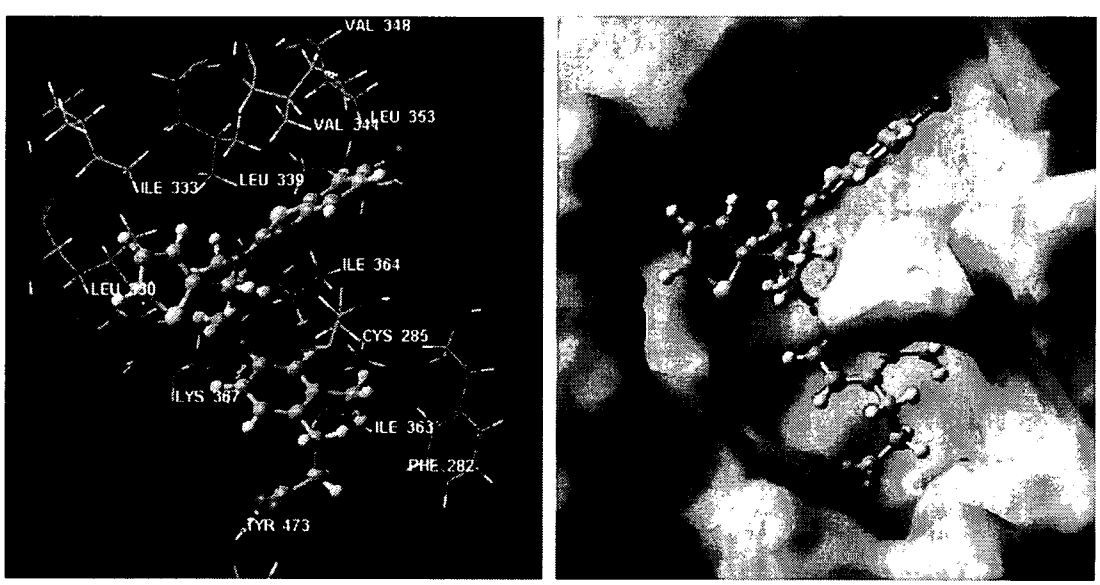

Figure 3. View of the conformation of **17** docked in PPARδ. Amino acid residues and hydrogen bonds are displayed as wires and dotted lines, respectively (left), and the surface of the PPARδ is displayed in the background (right).

and compounds **6** and **11** also showed selectivity towards PPARδ.

Having investigated the requirements for the R^1 group, we next turned our attention to the benzothiazole ring. The R^1 group was fixed as the benzyl group and the effect of a substituent at the 6-position of the benzothiazole ring (R^2 group) was examined. Among compounds **6**, **12**, and **13**, compound **12** (R^2 = Cl) showed transcriptional activity for PPARδ more potently than compound **6**, whereas methyl compound **13** displayed activity similar to **6**.

We also examined the effect of linker length. Compound **14**, where X = CH_2CH_2, modestly improved the PPARδ activity of compound **6**, where X = CH_2.

Since earlier studies revealed that the introduction of a methyl group at the *ortho* position of phenylpropanoic acid improved potency and selectivity toward PPARδ,[26,27] we looked at the effects of the R^3 group. The introduction of a methyl substituent at the *ortho* position of phenylpropanoic acid led to a 2.5-fold increase of PPARδ activity (**6** vs **15**). On the other hand, the introduction of ethyl substitution (compound **16**) was not effective.

Encouraged by these findings, we prepared compound **17** with the best combination of R^1–R^3 and X groups in this study. To our satisfaction, compound **17** showed the highest activity and selectivity for PPARδ in this series.[28]

Next, we studied the binding mode of compound **17**, the most active compound in this study, using Glide 3.5 and Macromodel 8.1 software.[29] As expected, inspection of the simulated PPARδ/**17** complex suggested that compound **17** had a Y-shaped conformation and filled the Y-shaped pocket of PPARδ appropriately (Fig. 3). Specifically, the 6-Cl-benzothiazole ring and the thiophene ring are estimated to occupy each of the two legs of the Y-shaped pocket which are formed by Val 341, Cys, 285, Val 348 and by Leu 330, Ile 333, Leu 339, respectively. In addition, it was shown that the Me group of **17** is located in the small hydrophobic pocket composed of Phe 282, Cys 285, and Ile 363. Interestingly, a hydrogen bond was observed between the oxygen atom of the ether linker and Lys 367. This hydrogen bond may be another important factor for PPARδ selectivity, because no such hydrogen bond has been observed between phenylpropanoic acid derivatives and PPARα or PPARγ.[13,14,30]

In summary, to explore novel PPARδ-selective agonists, we designed and prepared a series of phenylpropanoic acid derivatives. Compound **6** bearing a benzothiazole ring and a benzyl group showed PPARδ activity and selectivity. The introduction of a Cl group at the C-6 position of the benzothiazole ring and Me group at the *ortho* position of phenylpropanoic acid further improved PPARδ transcriptional activity. Compound **17**, which has the best R^1–R^3 and X groups, was found to be the most potent and selective PPARδ agonist in this series. Molecular modeling suggested that compound **17** fills the Y-shaped pocket of PPARδ appropriately. Currently, further detailed studies pertaining to compound **17** are under way.

References and notes

1. Willson, T. M.; Brown, P. J.; Sternbach, D. D.; Henke, B. R. *J. Med. Chem.* **2000**, *43*, 527.
2. Staels, B.; Dallongeville, J.; Auwerx, J.; Schoonjans, E.; Leitersdorf, E.; Fruchart, J.-C. *Circulation* **1998**, *98*, 2088.
3. Way, J. M.; Harrington, W. W.; Brown, K. K.; Gottschalk, W. K.; Sundseth, S. S.; Mansfield, T. A.; Ramachandran, R. K.; Willson, T. M.; Kliewer, S. A. *Endocrinology* **2001**, *142*, 1269.
4. Forman, B. M.; Chen, J.; Evans, R. M. *Proc. Natl. Acad. Sci. U.S.A.* **1997**, *94*, 4312.
5. Cantello, B. C. C.; Cawthorone, M. A.; Cottam, G. P.; Duff, P. T.; Haigh, D.; Hindley, R. M.; Lister, C. A.; Smith, S. A.; Thurlby, P. L. *J. Med. Chem.* **1994**, *37*, 3977.
6. Momose, Y.; Meguro, K.; Ikeda, H.; Hatanaka, C.; Oi, S.; Sohda, T. *Chem. Pharm. Bull.* **1991**, *39*, 1440.
7. Wang, Y.-X.; Lee, C.-H.; Tiep, S.; Yu, R. T.; Ham, J.; Kang, H.; Evans, R. M. *Cell* **2003**, *113*, 159.
8. Wang, Y.-X.; Zhang, C.-L.; Yu, R. T.; Cho, H. K.; Nelson, M. C.; Bayuga-Ocampo, C. R.; Ham, J.; Kang, H.; Evans, R. M. *PloS. Biol.* **2004**, *2*, 1532.
9. Leibowitz, M. D.; Fievet, C.; Hennuyer, N.; Peinado-Onsurbe, J.; Duez, H.; Berger, J.; Cullinan, C. A.; Sparrow, C. P.; Baffic, J.; Berger, G. D.; Santini, C.; Marquis, R. W.; Tolman, R. L.; Smith, R. G.; Moller, D. E.; Auwerx, J. *FEBS Lett.* **2000**, *473*, 333.
10. Tanaka, T.; Yamamoto, J.; Iwasaki, S.; Asaba, H.; Hamura, H.; Ikeda, Y.; Watanabe, M.; Magoori, K.; Ioka, R. X.; Tachibana, K.; Watanabe, Y.; Uchiyama, Y.; Sumi, K.; Iguchi, H.; Ito, S.; Doi, T.; Hamakubo, T.; Naito, M.; Auwerx, J.; Yanagisawa, M.; Kodama, T.; Sakai, J. *Proc. Natl. Acad. Sci. U.S.A.* **2003**, *100*, 15924.
11. Graham, T. L.; Mookherjee, C.; Suckling, K. E.; Palmer, C. N. A.; Patel, L. *Atherosclerosis* **2005**, *181*, 29.
12. Lee, C.-H.; Chawla, A.; Urbiztondo, N.; Liao, D.; Boisvert, W. A.; Evans, R. M. *Science* **2003**, *302*, 453.
13. Although compound **1** showed weak transactivation activity for PPARγ (Fig. 2), it displayed high affinity to PPARγ in a binding assay (Ref. 14,15).
14. Usui, S.; Suzuki, T.; Hattori, Y.; Etoh, K.; Fujieda, H.; Nishizuka, M.; Imagawa, M.; Nakagawa, H.; Kohda, K.; Miyata, N. *Bioorg. Med. Chem. Lett.* **2005**, *15*, 1547.
15. Usui, S.; Fujieda, H.; Suzuki, T.; Yoshida, N.; Nakagawa, H.; Miyata, N. *Bioorg. Med. Chem. Lett.* **2006**, *16*, 3249.
16. Fukuyama, T.; Jow, C.-K.; Cheung, M. *Tetrahedron Lett.* **1995**, *36*, 6373.
17. Fukuyama, T.; Cheung, M.; Jow, C.-K.; Hidai, Y.; Kan, T. *Tetrahedron Lett.* **1997**, *38*, 5831.
18. Mitsunobu, O. *Synthesis* **1981**, 1.
19. Wagaw, S.; Buchwald, S. L. *J. Org. Chem.* **1996**, *61*, 7240.
20. Maryanoff, B. E.; Reitz, A. B. *Chem. Rev.* **1989**, *89*, 863.
21. Li, T.; Fujita, Y.; Tsuda, Y.; Miyazaki, A.; Ambo, A.; Sasaki, Y.; Jinsmaa, Y.; Bryant, S. D.; Lazarus, L. H.; Okada, Y. *J. Med. Chem.* **2005**, *48*, 586.
22. Beletskaya, I. P.; Cheprakov, A. V. *Chem. Rev.* **2000**, *100*, 3009.
23. Fukuen, S.; Iwaki, M.; Yasui, A.; Makishima, M.; Matsuda, M.; Shimomura, I. *J. Biol. Chem.* **2005**, *280*, 23653.
24. Human embryonic kidney (HEK) 293 cells were cultured in DMEM containing 5% fetal bovine serum at 37 °C in a humidified atmosphere of 5% CO_2 in air. Transfections of PPAR and reporter gene con-

structs were performed by calcium phosphate coprecipitation. Eight hours after transfection, ligands were added. Cells were harvested 12–16 h after treatment, and luciferase and β-galactosidase activities were assayed using a 1420 ARVO^{TM} MX multilabel counter (Perkin-Elmer, Boston, MA, U.S.A.). DNA cotransfection experiments included 58 ng of reporter plasmid, 12 ng of CMX-β-galactosidase, and 18 ng of each receptor expression plasmid per well in a 96-well plate. Luciferase data were normalized to an internal β-galactosidase control and reported values are means of triplicate assays.

25. Xu, H. E.; Lambert, M. H.; Montana, V. G.; Parks, D. J.; Blanchard, S. G.; Brown, P. J.; Sternbach, D. D.; Lehmann, J. M.; Wisely, G. B.; Willson, T. M.; Kliewer, S. A.; Milburn, M. V. *Mol. Cell* **1999**, *3*, 397.
26. Epple, R.; Azimioara, M.; Russo, R.; Bursulaya, B.; Tian, S.-S.; Gerken, A.; Iskandar, M. *Bioorg. Med. Chem. Lett.* **2006**, *16*, 2969.
27. Weigand, S.; Bischoff, H.; Dittrich-Wengenroth, E.; Heckroth, H.; Lang, D.; Vaupel, A.; Woltering, M. *Bioorg. Med. Chem. Lett.* **2005**, *15*, 4619.
28. The relative efficacy of compound **17** was 86% of that of GW501516.
29. The X-ray structure of PPARδ complexed with GW2433 (PDB code 1GWX) was used as the target structure for docking. Protein preparation, receptor grid generation and ligand docking were performed using the software Glide 3.5. Compound **17** was docked into the ligand binding site of PPARδ. The extra precision mode of Glide was used to determine favorable binding poses, which allowed the ligand conformation to be flexibly explored while holding the protein as a rigid structure during docking. The predicted complex structure was then fully energy-minimized with both the protein and the ligand allowed to move using Macromodel 8.1 software. The conformation of **17** in the PPARδ ligand binding site was minimized by MM calculation based upon the OPLS-AA force field with each parameter set as follows; solvent: water, method: LBFGS, Max # Iterations: 10,000, Converge on: Gradient, Convergence Threshhold: 0.05.
30. Gampe, R. T., Jr.; Montana, V. G.; Lambert, M. H.; Miller, A. B.; Bledsoe, R. K.; Milburn, M. V.; Kliewer, S. A.; Willson, T. M.; Xu, H. E. *Mol. Cell* **2000**, *5*, 545.

Highlighted paper selected by Editor-in-chief

Nitration of Specific Tyrosine Residues of Cytochrome c Is Associated with Caspase-Cascade Inactivation

Hidehiko NAKAGAWA,*[a] Nobuko KOMAI,[b] Mitsuko TAKUSAGAWA,[b] Yuri MIURA,[c] Tosifusa TODA,[c] Naoki MIYATA,[a] Toshihiko OZAWA,[b] and Nobuo IKOTA[b]

[a] *Department of Organic and Medicinal Chemistry, Graduate School of Pharmaceutical Sciences, Nagoya City University; Nagoya 467–8603, Japan:* [b] *Redox Regulation Research Group, National Institute of Radiological Sciences; Chiba 263–8555, Japan: and* [c] *Tokyo Metropolitan Institute of Gerontology; Tokyo 173–0015, Japan.*
Received August 10, 2006; accepted October 17, 2006; published online October 19, 2006

Peroxynitrite, a potent oxidative stress inducer, inhibits the mitochondrial electron transfer, induces cell death, and is considered to be involved in the pathology of various diseases. However, the intracellular mechanisms involved in the cell death process are not fully understood. Here we demonstrate that the enhanced nitration of specific tyrosine residues of cytochrome c, which are induced by continuous peroxynitrite exposure, attenuates cytochrome c-induced caspase-9 activation *in vitro*. Interestingly, cytochrome c nitrated with a single high dose of peroxynitrite preserved its potency, while this did not occur when cytochrome c was treated with continuous peroxynitrite exposure. Although both of these experiments resulted in cytochrome c nitration at the tyrosine residues, it was found that nitration at specific residues was enhanced only when cytochrome c was exposed to continuous peroxynitrite. This is the first report to demonstrate that cytochrome c nitration affects the apoptotic pathway by means of enhancement of nitration at specific tyrosine residues. This result implies that the nitration pattern of cytochrome c may affect the efficacy of the mitochondrial pathway in apoptotic cell death.

Key words cytochrome c; nitrotyrosine; apoptosis; peroxynitrite; caspase

Peroxynitrite is a very strong oxidant, and is considered a candidate as an *in vivo* oxidant for inducing the oxidative and "nitrative" stress in various diseases, such as cardiovascular disease,[1—3] brain ischemia,[4—7] Parkinson's disease,[8—10] Alzheimer's disease,[11—14] amyotrophic lateral sclerosis,[15,16] other neurodegenerative diseases,[17,18] and sepsis.[19,20] Peroxynitrite causes nitration of free tyrosine and protein tyrosine residues. Although this reaction has been considered as the "footprint" of peroxynitrite production, it is not exclusively caused by peroxynitrite, but formed by the reaction of nitrite with hydrogen peroxide in the presence of myeloperoxidase.[21] Nonetheless, protein tyrosine nitration is a clue that reactive nitrogen species (RNS), like peroxynitrite and its equivalents, are produced and that the biological system has been damaged by RNS stresses. Some reports indicate that the nitration of protein tyrosine residues can cause some changes in function. Radi and colleagues reported that cytochrome c was nitrated at a specific tyrosine residue by a bolus peroxynitrite treatment depending on the concentration of peroxynitrite.[22] According to their results, nitration of cytochrome c resulted in loss of function as an ascorbate oxidase and in the downregulation of the oxygen consumption in mitochondrial preparation. We also independently reported that the nitration of a single tyrosine residue in cytochrome c by a relatively low dose of peroxynitrite resulted in the upregulation of its peroxidase activity for hydrogen peroxide and in the actual impairment of the membrane potential formation, which is important for ATP synthesis, in isolated mitochondrial preparations.[23]

It is well known that cytochrome c plays an important role in mitochondria-dependent apoptotic cell death. As a response to apoptotic stimuli, cytochrome c is released from the intermembrane space to the cytosol, and forms the apoptosome complex with procaspase-9 and Apaf-1 to activate caspase-9 and the downstream caspases, resulting in apoptotic death execution. One report[24] investigated the effect of cytochrome c treated with a bolus of peroxynitrite on the apoptotic cascades. In that report, cytochrome c nitrated with a bolus treatment of peroxynitrite retained its ability for caspase activation. Under the pathophysiological conditions, however, peroxynitrite production was assumed to be relatively low and sustained. The effect of low-dose and continuous exposure of cytochrome c to peroxynitrite on caspase activation was not evaluated, and the relationship between cytochrome c nitration and the caspase cascade activation has not been well investigated.

Here, we report on the nitration of cytochrome c by various methods of peroxynitrite exposure, and we analyze the relationship between tyrosine nitration and the ability of cytochrome c to cause caspase cascade activation *in vitro*. We determined that the modification pattern of cytochrome c was dependent on the duration and concentration of peroxynitrite exposure, and that cytochrome c nitration by continuous exposure to peroxynitrite attenuated its potency for caspase 9 activation. However, cytochrome c nitration by a bolus peroxynitrite treatment did not change that ability.

MATERIALS AND METHODS

Chemicals Cytochrome c (bovine heart), aprotinin, and pepstatin A were purchased from Sigma (St. Louis, MO, U.S.A.). Pronase was from Boehringer-Mannheim (Mannheim, Germany). 3-Nitro-L-tyrosine, 5-methoxytryptamine and tetranitromethane (TNM) were from Aldrich (Milwaukee, WI, U.S.A.). Staurosporine and leupeptin were purchased from Wako Pure Chemical Industries Ltd. (Osaka, Japan). PMSF was from Nacalai Tesque (Kyoto, Japan). 3-Morpholinosydnonimine (SIN-1) was from Dojindo (Kumamoto, Japan). All other reagents were from Sigma, Bio-Rad (Hercules, CA, U.S.A.), or Amersham Biosciences

* To whom correspondence should be addressed. e-mail: deco@phar.nagoya-cu.ac.jp
© 2007 Pharmaceutical Society of Japan

Corp. (Piscataway, NJ, U.S.A.) All the reagents were of analytical or biochemical grade.

Peroxynitrite Preparation Peroxynitrite was synthesized as an alkaline solution based on the method of Pryor *et al.*[23,25] The solution was stored at −80 °C until use. The concentration of the peroxynitrite solution was determined spectrophotometrically by measuring the absorbance at 302 nm (ε=1670 $M^{-1}cm^{-1}$). Using this method, up to a 500 mM solution of peroxynitrite was obtained. The concentration of the stock solution was determined again before use, and then the stock was diluted to the desired concentration with 0.01 M NaOH on an ice bath.

Cell Culture A C6 rat glioma cell line was purchased from American Type Culture Collection (ATCC, Manassas, VA, U.S.A.) and cultured in Ham's F10 medium containing penicillin and streptomycin, supplemented with horse serum and fetal bovine serum as described in the ATCC instruction. The cells were maintained at 37 °C in a humidified 5% (v/v) CO_2 incubator under a sub-confluent condition.

Preparation of Peroxynitrite- and TNM-Treated Cytochrome c Cytochrome c solution (20 μM) was prepared in PBS. For continuous treatment with peroxynitrite, 1 μl of 50 mM peroxynitrite in 0.01 M NaOH was repeatedly added to 1 ml of the cytochrome c solution (20 μM) 20 times at 30-s intervals while mixing. Because peroxynitrite is unstable and reactive at neutral pH, it is practically fully reacted or decomposed within 30 s after addition. For a continuous infusion, 20 μl of 50 mM peroxynitrite in 0.01 M NaOH was continuously infused into 1 ml of the cytochrome c solution over 20 min with a syringe pump while mixing. For a single treatment with peroxynitrite, 20 μl of 50 mM peroxynitrite was added to the cytochrome c solution all at once. For a low-dose single or control treatment, 1 μl of 50 mM peroxynitrite or no peroxynitrite was added to the cytochrome c solution containing decomposed peroxynitrite equivalent to the 19 μl or 20 μl of 50 mM peroxynitrite, respectively. After the addition of 20 μl of peroxynitrite solution, the resulting solution was confirmed to be neutral (pH 7 to 8). All the peroxynitrite-treated cytochrome c solutions were subjected to gel filtration with Sephadex G-25, or centrifugal concentration and wash with a membrane filter (polyethylenesulfonate, 5000 molecular weight cut off, Vivascience AG, Hanover, Germany). The cytochrome c concentrations were adjusted according to the absorbance at 409 nm. With the peroxynitrite treatment at the concentration range in these experiments, the maximum absorbance and wavelength of the Soret band (409 nm) showed almost no changes. The Soret band was slightly blue-shifted by less than 1 nm in wavelength. A solution of cytochrome c repeatedly treated with low-dose peroxynitrite in the presence of 5-methoxytryptamine (5MT) was also prepared in order to determine the inhibitory effect of 5MT.

For the TNM treatment, 1 mM cytochrome c in PBS was diluted with 10 mM sodium phosphate buffer (pH 8.0) to prepare 1 ml of 20 μM cytochrome c. To this solution, 1.19 μl of 10% (v/v) TNM solution in ethanol was added, and mixed vigorously for 1 h at room temperature. The reaction was terminated by gel filtration through Sephadex G-25 with PBS, and the concentration of cytochrome c was adjusted according to the absorbance at 409 nm.

In Vitro* Caspase Activation Assay** The caspase activation assay in a cell-free system was carried out using a cytosolic fraction of C6 cells and exogenous cytochrome c.[26,27] Intact C6 cells were gently washed and harvested by scraping in PBS. The collected cells were washed with PBS again and precipitated at 200 ***g for 5 min at room temperature. The cells were then resuspended in 3 times the volume of buffer A (250 mM sucrose, 20 mM Hepes-K [pH 7.5], 10 mM KCl, 1.5 mM $MgCl_2$, 1 mM EDTA, 1 mM EGTA, 1 mM dithiothreitol) supplemented with 4 μg/ml leupeptin, 2 μg/ml pepstatin A, 2 μg/ml aprotinin, 0.1 mM PMSF, and 25 μg/ml *N*-acetyl-leucyl-leucyl-norleucine. The suspension was incubated on an ice bath for 15 min, and then the cells were homogenized with a glass homogenizer with 3 to 5 strokes of a pestle, or gently passed through a 22-gauge needle 15 times. The resulting cell homogenate was centrifuged at 7700 ***g*** and the supernatants were subsequently centrifuged at 100000 ***g*** for 30 min at 4 °C. The supernatant was collected as a cytosolic fraction (S-cytosol). The S-cytosol fraction did not contain cytochrome c, as confirmed by immunoblotting with the anti-cytochrome c antibody (1 : 1000 dilution, mouse IgG clone 7H8.2C12, BD Biosciences, San Jose, CA, U.S.A.). The protein concentrations of the obtained S-cytosol fractions ranged from 2.5 to 5 mg protein/ml.

For *in vitro* caspase activation assay, the peroxynitrite-treated or control cytochrome c (800 nM) was added to the S-cytosol fraction (2.5 mg protein/ml) with or without addition of 0.5 mM ATP. The mixture was incubated at 30 °C for 90 min, and the proteins were denatured by boiling for 10 min in a SDS sample buffer. The samples were subsequently subjected to SDS-PAGE (15% gel) and immunoblotting with the anti-cleaved caspase-3 antibody (1 : 1000 dilution, Cell Signaling Technology, Inc., Danvers, MA, U.S.A.) and visualized by chemiluminescence with ECL-plus reagents (Amersham Biosciences Corp., Piscataway, NJ, U.S.A.).

Detection of Nitrotyrosine in Hydrolysate of Peroxynitrite-Treated Cytochrome c Peroxynitrite-treated cytochrome c was hydrolyzed enzymatically as reported previously.[23] The hydrolysate of peroxynitrite-treated cytochrome c was centrifuged at 175 ***g*** for 2 min, and the supernatant was analyzed by HPLC with a multi-wavelength detector (JASCO Co., Ltd., Tokyo, Japan) and an octadecylsilyl (ODS) column (TSK-GEL ODS-80Ts, 4.6×150 mm, Tosoh, Tokyo, Japan). As a mobile phase, 0.1 M potassium phosphate buffer (pH 3.5) containing 5% (v/v) methanol was used. The elution of tyrosine and nitrotyrosine was confirmed by comparison of the retention time with the authentic compounds.

HPLC and Mass Spectral Measurement of Tryptic Peptides from Nitrated Cytochrome c Peroxynitrite-treated cytochrome c (20 μM) was concentrated with a centrifugal concentrator with a polyethylenesulfonate membrane and molecular weight cut-off at 5000. The concentrated cytochrome c was washed once by a centrifugal concentrator with an ammonium carbonate solution (0.1 M, pH 8.0), and adjusted to 1.28 mM with the washing solution. A proteomic grade of trypsin (Sigma, St. Louis, MO, U.S.A.) was reconstituted with 1 mM HCl according to the manufacturer's instruction and added to the cytochrome c solution at a ratio of 1 : 100 (w/w) as the amount of proteins. The mixture was incubated at 37 °C for 16 h for tryptic digestion. The obtained tryptic peptides were analyzed with matrix-associated laser

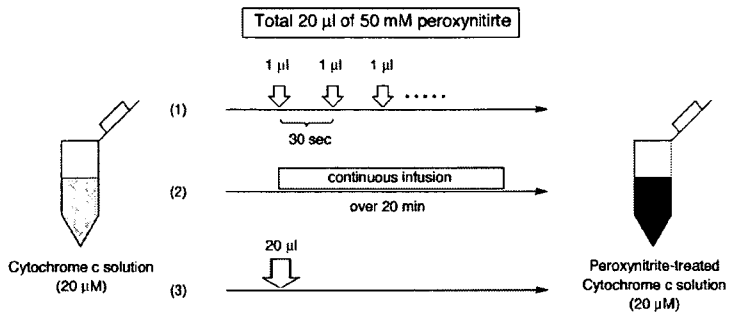

Treatment	#	peroxynitrite stock solution (50 mM) vol./add.	No. of add.	Interval
Continuous treatment (CT)				
Continuous treatment	(1)	50 mM x 1 μl	20	30 sec
Continuous infusion	(2)	50 mM x 20 μl	(infusion over 20 min)	
Bolus treatment (BT)	(3)	50 mM x 20 μl	1	-

Chart 1. Preparation of Peroxynitrite-Treated Cytochrome c

dissorption ionization-time of flight mass spectrometry (MALDI-TOFMS), and the mass data were searched for peptide mass finger-printing databases to confirm the appropriate digestion of cytochrome c protein. Furthermore, the digested tryptic peptides were also subjected to a reversed-phase HPLC analysis with a linear gradient of 0 to 45% (v/v) acetonitrile in 0.1% (v/v) trifluoroacetic acid in 60 min, by monitoring with a multi-wavelength detector. The eluted peptide fractions were collected and lyophilized. Each fraction was reconstituted with H_2O/acetonitrile (8 : 2) and analyzed with MALDI-TOFMS. The digested peptide fragments were compared for the observed mass data for each fragment with the calculated mass numbers of the possible tryptic peptide fragments. The tyrosine-, nitrotyrosine-, and tryptophan-containing peptides were compared by the absorption spectra of the peptide fragments obtained from the HPLC analysis with a multi-wavelength detector.

RESULTS

Nitration of Cytochrome c by Continuous Peroxynitrite Infusion *in Vitro* We prepared peroxynitrite-treated cytochrome c in two different ways. One was a continuous infusion of peroxynitrite into cytochrome c in Earle's balanced salt solution (EBSS), and the other was a bolus treatment of cytochrome c with peroxynitrite. Cytochrome c treated with a continuous addition of peroxynitrite solution at 1-min intervals was also prepared. The cumulative final concentration of peroxynitrite was the same in all treatments. In all the preparations of peroxynitrite-treated cytochrome c, tyrosine nitration was confirmed by the detection of 3-nitrotyrosine in the pronase-digested hydrolysates of treated cytochrome c by an HPLC analysis of aromatic amino acid (Fig. 1).

To address the difference in the nitration sites between both nitrated cytochrome c preparations, the continuous and bolus peroxynitrite-treated cytochrome c were subjected to trypsin digestion, HPLC analysis, and MALDI-TOF mass spectrometry. The tryptic peptides of either continuous or bolus peroxynitrite-treated cytochrome c were first resolved by HPLC (Fig. 2). The chromatogram monitoring at 364 nm,

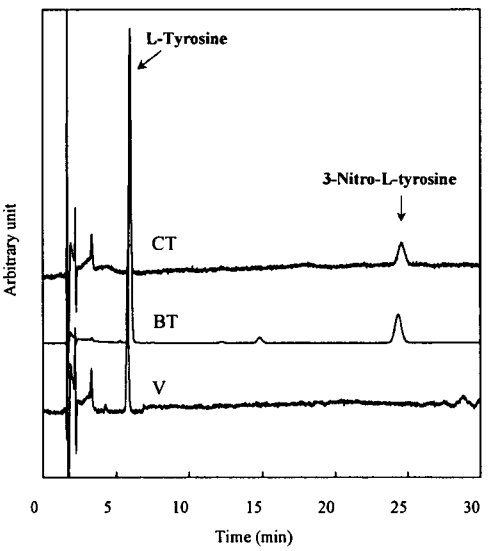

Fig. 1. Detection of Nitrotyrosine in Peroxynitrite-Treated Cytochrome c

Peroxynitrite-treated cytochrome c was hydrolyzed enzymatically, and subjected HPLC analysis for detection of nitrotyrosine. The labels CT, BT, and V on the chromatograms indicate the cytochrome c samples with the continuous, single-dose (bolus), and control (vehicle) treatment of peroxynitrite, respectively.

which is a local absorption maximum wavelength in nitrotyrosine, revealed that 4 peptide fragments contained nitrotyrosine residues in both groups treated with continuous and bolus treatment of peroxynitrite. The chromatogram at 215 nm revealed that the 3 peptide peaks (a, c, i) decreased with peroxynitrite treatment, concomitantly with the increase of the nitrated peptide peaks (b, d, g, j), without any changes in the other tryptic peptides in the chromatogram. Furthermore, from the spectra of these decreasing peaks, it was also confirmed that these peptides contained tyrosine residues. The fractionated tryptic peptides, including tyrosine- and nitrotyrosine-containing peptides, were subjected to a MALDI-TOF mass spectrometer and analyzed with both peptide mass fingerprinting from the public databases and the peptide molecular masses measured. From these results, it was revealed that at least 3 of the 4 tyrosine residues (Y48, Y67, Y74) in

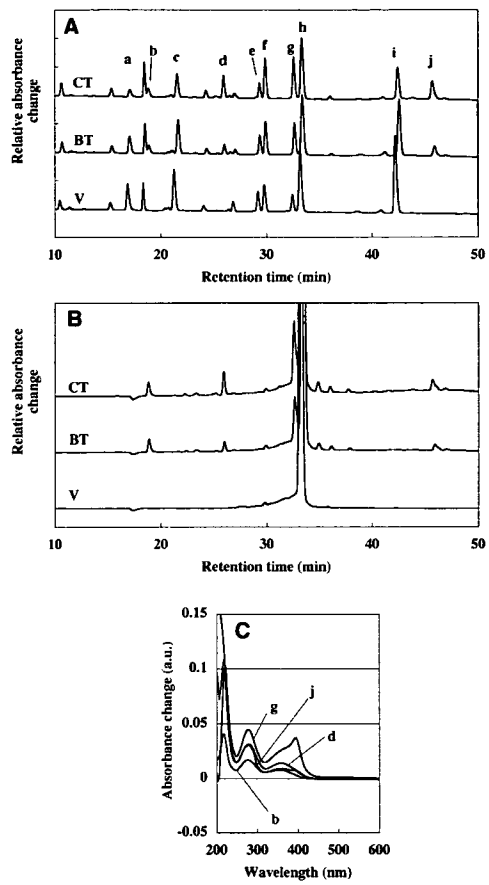

Fig. 2. Chromatogram and Absorption Spectra of the Tryptic Peptides of Peroxynitrite-Exposed Cytochrome c

Cytochrome c treated with peroxynitrite was dialyzed against ammonium carbonate, and digested with a sequencing grade of trypsin for 16 h at 37 °C. The resulting tryptic peptides were separated by HPLC with an ODS column and detected with a multi-wavelength absorption detector. A: chromatograms at 215 nm, B: chromatograms at 364 nm, C: absorption spectra of the nitrated peptide peaks. Small letter alphabetic labels on the peptide peaks and spectra correspond to the labels shown in Table 1. The labels CT, BT, and V on the chromatograms indicate the cytochrome c samples with the continuous, single-dose (bolus), and control (vehicle) treatment of peroxynitrite, respectively.

Table 1. Assignment of Tryptic Peptides Based on the Observed Mass Numbers in Mass Spectrometry

Tryptic peptide	Mass number		Peak label[a]
	Calculated	Observed	
$Y^{74}IPGTK^{79}$	677.76	678.08	a
$Y^{74}IPGTKMIFAGIK^{86}$-NO_2	1483.73	1485.25	d
$T^{28}GPNLHGLFGR^{38}$	1168.27	1168.56	e or f[b]
$T^{40}GQAPGFSY^{48}TDANK^{53}$	1456.44	1456.09	c
$T^{40}GQAPGFSY^{48}TDANK^{53}$-$NO_2$	1501.44	1501.44	d
$E^{92}DLIAY^{97}LKKATNE^{104}$	1507.63	1504.48	g[c]
$I^{9}FVQKCAQCHTVEK^{22}$	1633.89	1633.61	h[c]
$G^{56}ITWGEETLMEY^{67}LENPK^{72}$	2010.17	2009.56	i
$G^{56}ITWGEETLMEY^{67}LENPK^{72}$-$NO_2$	2055.17	2054.06	j

a) The letter indicates the corresponding peak label in the chromatogram shown in Fig. 2. *b*) Peak e and f could not be separately fractionated for the mass measurement. *c*) Assignment of peak g and peak h are also based on their absorption spectra in addition to this peptide mass measurement. Peak h showed a unique absorption around 400 nm based on the heme, which attaches to two cysteine residues of Cys14 and Cys17.

Table 2. Relative Nitrotyrosine Content in Peroxynitrite-Treated Cytochrome c

Treatment	Nitrated cytochrome c (%)[a]	Fold increase[c]
Continuous treatment (CT)	37.4±0.37[b]	1.6
Bolus treatment (BT)	23.4±0.27[b]	1
Vehicle (V)	0.70[c]	—

a) Percentage for cytochrome c with 3-nitrotyrosine: Since cytochrome c contains 4 tyrosine residues per molecule, the ratio (%) of nitrated cytochorme c were calculated by dividing the amount of 3-nitrotyrosine by 1/4 amount of total tyrosine. *b*) Mean±S.D. from three independent experiments. *c*) Potency of a continuous treatment for nitration compared with that of a bolus treatment.

Table 3. Relative Nitration of Tyrosine 74 Containing Peptide

Treatment	Relative nitration[a]
Continuous treatment (CT)	4.25 (4.22, 4.27)[b]
Bolus treatment (BT)	1 (1.30, 0.70)[b]
Vehicle (V)	0.03 (0.05, 0.01)[b]

a) Relative amount of the nitrated peptide containing tyrosine 74 based on the amount of nitration by a bolus treatment. *b*) The value indicates the average of two independent experiments showing individual values in parentheses.

cytochrome c were nitrated without any detectable changes in the other peptide fragments under the conditions of the peroxynitrite treatment in this study (Fig. 2, Table 1). The peptide fragment containing tyrosine 74 (peak a in Fig. 2) was decreased by treatment of peroxynitrite, and the corresponding nitrated peptide (peak d in Fig. 2) was concomitantly increased. Although peak d also contained a certain amount of nitrated peptide containing tyrosine 48 (Table 1), it was found that the corresponding unnitrated fragment (peak c in Fig. 2) was only slightly decreased.

When we focused on the differences between the continuous and bolus peroxynitrite treatment, it was found that nitration at tyrosine 74 was specifically enhanced, and the nitration at tyrosine 67 was also slightly enhanced in cytochrome c with continuous treatment with peroxynitrite. The amount of nitrated cytochrome c (at any tyrosine residue) was 1.6 times larger by continuous treatment than by bolus treatment (Table 2). Whereas, nitration in tyrosine 74 is 4.2 times more frequent in continuously peroxynitrite-treated cytochrome c than in bolus peroxynitrite-treated (Table 3). There were no differences in the nitration at the other tyrosine residues (Fig. 2, Table 1). When peroxynitrite was infused over more than 4 h, cytochrome c nitration was not observed.

***In Vitro* Apoptosis Assay with Peroxynitrite-Exposed Cytochrome c** The ability of tyrosine-nitrated cytochrome c to cause caspase activation was evaluated by an *in vitro* apoptosis assay. Chemically modified cytochrome c was added to an intact cytosolic fraction from C6 cells and incubated at 30 °C for 90 min. For the detection of caspase activation, cleaved caspase-3 fragments (p17, p19) were observed *via* immunoblotting analysis with the specific antibody for the cleaved fragments of caspase-3. With the nitrated cytochrome c that had been continuously treated with peroxynitrite, caspase activation was not observed in the assay, while the activation was observed when the control and the intact cytochrome c preparations were used. With the TNM-treated cytochrome c, caspase activation was also attenuated (Figs. 2, 3). Interestingly, caspase activation was observed with the cytochrome c preparation treated with a bolus (1 mM) of peroxynitrite (Fig. 3). The activation was also observed with cytochrome c treated with a single low dose (50 μM) of perox-

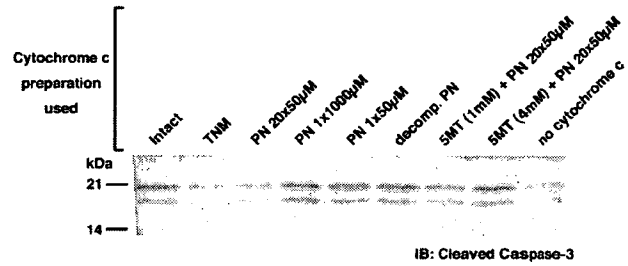

Fig. 3. Detection of Caspase-3 Fragments after *in Vitro* Caspase Activation Reaction with Exogenous Cytochrome c Nitrated by Continuous Peroxynitrite Treatment

Cytosolic fraction prepared from the intact cells was incubated with the cytochrome c preparations independently pretreated as indicated on the top of each lane. Caspase-3 active fragments (p17, p19) were observed with the specific antibody using chemiluminescence detection. TNM: tetranitromethane, PN: peroxynitrite, decomp. PN: decomposed PN, 5MT: 5-methoxytryptamine. PN 20×50 μM indicates 20 times of continuous treatment with 50 μM peroxynitrite. Representative data of the same results from three independent experiments are shown.

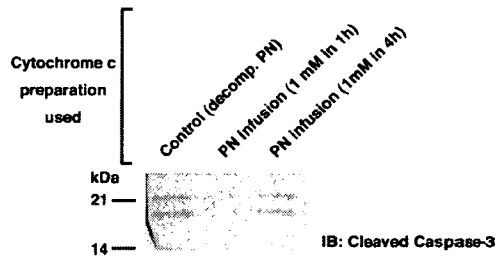

Fig. 4. Detection of Caspase-3 Fragments after the *in Vitro* Caspase Activation Reaction with the Exogenous Cytochrome c Nitrated by Continuous Peroxynitrite Exposure

Cytosolic fraction prepared from the intact cells was incubated with the cytochrome c preparations independently pretreated with peroxynitrite as indicated. The caspase-3 active fragments (p17, p19) were observed in the same way as in Fig. 3. PN: peroxynitrite, decomp. PN: decomposed PN, "PN 1 mM in 1 h" indicates that peroxynitrite was infused into the cytochrome c solution for 1 h, and the total cumulative concentration of peroxynitrite was 1 mM.

ynitrite. From these results, it was found that the ability of cytochrome c to induce the caspase cascade activation was attenuated by continuous or repeated peroxynitrite exposure, but not by a bolus treatment. For further investigation regarding whether this functional loss with continuous treatment of peroxynitrite depends on the nitration of cytochrome c or not, a nitration-specific peroxynitrite scavenger, 5-methoxytryptamine (5MT), was employed. 5MT has been found to inhibit tyrosine nitration by peroxynitrite without affecting the tyrosine-oxidizing activity.[28] In the presence of 5MT, cytochrome c was treated with peroxynitrite repeatedly, and this cytochrome c preparation was then subjected to an *in vitro* apoptosis assay. The result indicated that simultaneous 5MT treatment preserved the ability of cytochrome c to induce caspase activation with continuous peroxynitrite exposure (Fig. 4). Together with the results from the *in vitro* apoptosis assay, it was found that continuous exposure of peroxynitrite caused the nitration of cytochrome c and the attenuation of its ability for caspase activation. However, a bolus of peroxynitrite exposure did not show this effect, even though the treated cytochrome c was nitrated.

DISCUSSION

From the *in vitro* apoptosis assay, it was found that caspase cascade activation was suppressed when cytochrome c was treated with continuous peroxynitrite exposure, but this effect was not observed with a bolus treatment of peroxynitrite. We suggest that the attenuation of cytochrome c activity for caspase activation was closely related to tyrosine nitration because 5MT, a nitration-specific scavenger, preserved the activity of cytochrome c (Fig. 3). Our results from a bolus treatment of cytochrome c with peroxynitrite is consistent with a previous report,[24] in which cytochrome c treated with a bolus of peroxynitrite did not lose its ability for caspase cascade activation.

From the analysis of peroxynitrite-treated cytochrome c, it was found that all 4 positions of the tyrosine residues were nitrated in both methods of treatment. However, the tyrosine nitration at position 74 was increased when cytochrome c was exposed to continuous peroxynitrite treatment, compared with a bolus of peroxynitrite (Fig. 2, Table 1), although other tyrosine residues were nitrated to a similar extent with both treatments. By continuous treatment with peroxynitrite, the total amount of nitration to cytochrome c increased in some extent, but tyrosine 74 is more specifically nitrated by continuous treatment than by bolus treatment (Tables 2, 3). This suggests that continuous exposure of peroxynitrite is not only different from bolus one in the total amount of nitration, but also in the specificity of nitration. Based on the HPLC and MALDI-TOFMS analyses of the tryptic peptides of peroxynitrite-treated cytochrome c, methionine oxidation and modifications other than tyrosine nitration were not observed.

Our results suggest that the differential effect of continuous peroxynitrite exposure to cytochrome c on its potency for caspase activation depends on the extent of the nitration at tyrosine 74.

The tyrosine 74 residue is known to be important for the electron transfer reaction in mitochondria[29,30] and is located near the tyrosine 67 residue, which is the primary target for bolus peroxynitrite treatment.[22] Cytochrome c exposed to a low dose of peroxynitrite impaired electron transfer ability, as shown in our previous study.[23]

From the spectral analysis of nitrated cytochrome c, there was almost no difference between the nitrated and control cytochrome c except a slight (less than 2 nm) shift of the Soret band. This band shift may reflect a slight change of the coordination conditions. Additionally, HPLC and MALDI-TOF-MS analyses also suggest that there are no other detectable changes in the tryptic digest of the protein, except nitration of 3 tyrosine residues. Based on these observations, the differences between these 2 nitrated cytochrome c preparations can be attributed to the enhanced nitration of a specific tyrosine residue. These results implicate that the pattern of peroxynitrite exposure (continuous or bolus) results in different modifications at a specific tyrosine residue, and finally in different effects on caspase cascade activity. The redox status of cytochrome c is known to be involved in caspase activation. In this study, all the cytochrome c preparations, including the controls, were used in the oxidized form, as confirmed by the measurement of the absorption spectra of the samples. In this study, the mechanism of cytochrome c inactivation by peroxynitrite treatment was not fully revealed yet. It is known that cytochorme c interacts with apoptotic protease activating factor-1 (Apaf-1). It is possible that enhancement of Tyr 74 ni-

tration in cytochrome c may reduce its interaction with Apaf-1 or increase its dominant negative property. Although the molecular mechanisms of apoptosome inactivation by the specific nitration of cytochrome c still need to be clarified, our findings suggest that the nitration status at specific tyrosine residues can affect the ability of cytochrome c to cause capsase activation. It is known that cytochrome c interacts with Apaf-1 to form an active apoptosome complex. The enhanced nitration at tyrosine 74 may affect active apoptosome formation.

In conclusion, this study determined that cytochrome c nitrated by continuous treatment with peroxynitrite lost its ability to cause caspase cascade activation *in vitro*, whereas cytochrome c nitrated by a bolus peroxynitrite treatment had preserved activity. The differential property of the continuously peroxynitrite-exposed cytochrome c was closely related to the enhanced nitration of specific tyrosine residues. This is the first study to demonstrate that protein nitration at specific residues affects caspase activation. We suggest that the exposure pattern of peroxynitrite, including the duration and concentration, is important for cytochrome c activity for caspase activation.

Acknowledgments This work was supported in part by Grants-in-Aid for Scientific Research (No. 13771417 for H.N.) from the Ministry of Education, Culture, Sports, Science, and Technology, Japan.

REFERENCES

1) Virag L., Szabo E., Gergely P., Szabo C., *Toxicol. Lett.*, **140–141**, 113—124 (2003).
2) Ferdinandy P., Schulz R., *Br. J. Pharmacol.*, **138**, 532—543 (2003).
3) Ronson R. S., Nakamura M., Vinten-Johansen J., *Cardiovasc. Res.*, **44**, 47—59 (1999).
4) White B. C., Sullivan J. M., DeGracia D. J., O'Neil B. J., Neumar R. W., Grossman L. I., Rafols J. A., Krause G. S., *J. Neurol. Sci.*, **179**, (S 1—2), 1—33 (2000).
5) Ste-Marie L., Hazell A. S., Bemeur C., Butterworth R., Montgomery J., *Brain Res.*, **918**, 10—19 (2001).
6) Gursoy-Ozdemir Y., Bolay H., Saribas O., Dalkara T., *Stroke*, **31**, 1974—1980, discussion 1981 (2000).
7) Eliasson M. J., Huang Z., Ferrante R. J., Sasamata M., Molliver M. E., Snyder S. H., Moskowitz M. A., *J. Neurosci.*, **19**, 5910—5918 (1999).
8) Giasson B. I., Duda J. E., Murray I. V., Chen Q., Souza J. M., Hurtig H. I., Ischiropoulos H., Trojanowski J. Q., Lee V. M., *Science*, **290**, 985—989 (2000).
9) Good P. F., Hsu A., Werner P., Perl D. P., Olanow C. W., *J. Neuropathol. Exp. Neurol.*, **57**, 338—342 (1998).
10) Pennathur S., Jackson-Lewis V., Przedborski S., Heinecke J. W., *J. Biol. Chem.*, **274**, 34621—34628 (1999).
11) Castegna A., Thongboonkerd V., Klein J. B., Lynn B., Markesbery W. R., Butterfield D. A., *J. Neurochem.*, **85**, 1394—1401 (2003).
12) Luth H. J., Munch G., Arendt T., *Brain Res.*, **953**, 135—143 (2002).
13) Hensley K., Maidt M. L., Yu Z., Sang H., Markesbery W. R., Floyd R. A., *J. Neurosci.*, **18**, 8126—8132 (1998).
14) Smith M. A., Richey Harris P. L., Sayre L. M., Beckman J. S., Perry G., *J. Neurosci.*, **17**, 2653—2657 (1997).
15) Beal M. F., Ferrante R. J., Browne S. E., Matthews R. T., Kowall N. W., Brown R. H., Jr., *Ann. Neurol.*, **42**, 644—654 (1997).
16) Abe K., Pan L. H., Watanabe M., Kato T., Itoyama Y., *Neurosci. Lett.*, **199**, 152—154 (1995).
17) Duda J. E., Giasson B. I., Chen Q., Gur T. L., Hurtig H. I., Stern M. B., Gollomp S. M., Ischiropoulos H., Lee V. M., Trojanowski J. Q., *Am. J. Pathol.*, **157**, 1439—1445 (2000).
18) Aoyama K., Matsubara K., Fujikawa Y., Nagahiro Y., Shimizu K., Umegae N., Hayase N., Shiono H., Kobayashi S., *Ann. Neurol.*, **47**, 524—527 (2000).
19) Lanone S., Manivet P., Callebert J., Launay J. M., Payen D., Aubier M., Boczkowski J., Mebazaa A., *Biochem. J.*, **366**, 399—404 (2002).
20) Kooy N. W., Lewis S. J., Royall J. A., Ye Y. Z., Kelly D. R., Beckman J. S., *Crit. Care. Med.*, **25**, 812—819 (1997).
21) Sampson J. B., Ye Y., Rosen H., Beckman J. S., *Arch. Biochem. Biophys.*, **356**, 207—213 (1998).
22) Cassina A. M., Hodara R., Souza J. M., Thomson L., Castro L., Ischiropoulos H., Freeman B. A., Radi R., *J. Biol. Chem.*, **275**, 21409—21415 (2000).
23) Nakagawa H., Ohshima Y., Takusagawa M., Ikota N., Takahashi Y., Shimizu S., Ozawa T., *Chem. Pharm. Bull.*, **49**, 1547—1554 (2001).
24) Ueta E., Kamatani T., Yamamoto T., Osaki T., *Int. J. Cancer*, **103**, 717—722 (2003).
25) Pryor W. A., Cueto R., Jin X., Koppenol W. H., Ngu-Schwemlein M., Squadrito G. L., Uppu P. L., Uppu R. M., *Free Radic Biol. Med.*, **18**, 75—83 (1995).
26) Liu X., Kim C. N., Yang J., Jemmerson R., Wang X., *Cell*, **86**, 147—157 (1996).
27) Hampton M. B., Zhivotovsky B., Slater A. F., Burgess D. H., Orrenius S., *Biochem. J.*, **329**, 95—99 (1998).
28) Nakagawa H., Sumiki E., Ikota N., Matsushima Y., Ozawa T., *Antioxid. Redox. Signal*, **1**, 239—244 (1999).
29) Takano T., Kallai O. B., Swanson R., Dickerson R. E., *J. Biol. Chem.*, **248**, 5234—5255 (1973).
30) Takano T., Trus B. L., Mandel N., Mandel G., Kallai O. B., Swanson R., Dickerson R. E., *J. Biol. Chem.*, **252**, 776—785 (1977).

Leukemia (2007), 1–10
© 2007 Nature Publishing Group All rights reserved 0887-6924/07 $30.00
www.nature.com/leu

ORIGINAL ARTICLE

Proteome analyses of the growth inhibitory effects of NCH-51, a novel histone deacetylase inhibitor, on lymphoid malignant cells

T Sanda[1,2], T Okamoto[1], Y Uchida[1], H Nakagawa[3], S Iida[2], S Kayukawa[2], T Suzuki[3], T Oshizawa[4], T Suzuki[4], N Miyata[3] and R Ueda[2]

[1]*Department of Molecular and Cellular Biology, Nagoya City University Graduate School of Medical Sciences, Nagoya, Japan;* [2]*Department of Internal Medicine and Molecular Science, Nagoya City University Graduate School of Medical Sciences, Nagoya, Japan;* [3]*Department of Organic and Medicinal Chemistry, Nagoya City University Graduate School of Pharmaceutical Sciences, Nagoya, Japan and* [4]*Department of Cellular and Gene Therapy Products, National Institute of Health Sciences, Tokyo, Japan*

Recent reports showing successful inhibition of cancer and leukemia cell growth using histone deacetylase inhibitor (HDACi) compounds have highlighted the potential use of HDACi as anti-cancer agents. However, high incidence of toxicity and low stability *in vivo* were observed with hydroxamic acid-based HDACi such as suberoylanilide hydroxamic acid (SAHA), thus limiting its clinical applicability. In this study, we found that a novel non-hydroxamate HDACi NCH-51 could inhibit the cell growth of a variety of lymphoid malignant cells through apoptosis induction, more effectively than SAHA. Activation of caspase-3, -8 and -9, but not -7 was detected after the treatment with NCH-51. Gene expression profiles showed that NCH-51 and SAHA similarly upregulated *p21* and downregulated anti-apoptotic molecules including *survivin*, *bcl-w* and *c-FLIP*. Proteome analysis using two-dimensional electrophoresis revealed that NCH-51 upregulated anti-oxidant molecules including peroxiredoxin 1 and 2 and glutathione *S*-transferase at the protein level. Interestingly, NCH-51 induced reactive oxygen species (ROS) after 8 h whereas SAHA continuously declined ROS. Pretreatment with an antioxidant, *N*-acetyl-L-cysteine, abolished the cytotoxicity of NCH-51. These findings suggest that NCH-51 exhibits cytotoxicity by sustaining ROS at the higher level greater than SAHA. This study indicates the therapeutic efficacy of NCH-51 and novel insights for anti-HDAC therapy.
Leukemia advance online publication, 9 August 2007;
doi:10.1038/sj.leu.2404902
Keywords: histone deacetylase; apoptosis; reactive oxygen species; peroxiredoxin

Introduction

Histone deacetylase (HDAC) is responsible for deacetylation of histone or non-histone substrates.[1–3] Deacetylation of histone converts local chromatin into repressive configuration, resulting in the transcriptional repression.[2,3] The aberrant recruitment of HDAC is closely associated with leukemogenesis through silencing of expression of the genes involved in hematopoietic cell differentiation.[4] In addition, subsequent studies demonstrated that the malignant phenotypes of solid tumors could be ascribed to the aberrant activation of HDAC and deacetylation of the histone proteins adjacent to tumor suppressor genes.[5,6] Thus, a number of small-molecule HDAC inhibitors (HDACi) have been developed as anti-cancer agents.[1,7] In fact, HDACi compounds were shown to induce cell cycle arrest, differentiation and apoptosis in a variety of malignant cells.[1,7]

Suberoylanilide hydroxamic acid (SAHA) (also known as vorinostat) belongs to a hydroxamic acid-based hybrid polar compound and is a prototypic compound of HDACi.[7] Phase I clinical trials with refractory solid tumors and hematological malignancies by SAHA revealed frequent toxicities including dehydration, fatigue, diarrhea, anorexia and cytopenia, in spite of significant clinical benefits.[8] In addition, a poor pharmacokinetics of SAHA was noted.[8] Other hydroxamic acid-based derivatives showed similar therapeutic profiles.[9,10] Thus, we have attempted to develop a non-hydroxamate HDACi to overcome these problems. A novel HDACi NCH-51 was designed based on SAHA by replacement of the hydroxamic acid by acylated thiol group. NCH-51 could inhibit HDACs as strongly as SAHA and inhibited the cell growth of various solid tumor cell lines *in vitro* (mean IC_{50} values of NCH-51 and SAHA are 3.8 and 3.7 μM, respectively).[11] Unlike SAHA, NCH-51 is stable in human plasma at the remaining rate of approximately 51% after 24 h of administration (unpublished data).

Recent findings suggest that HDACi may have additional effects other than transcriptional interference. Although it is well established that HDACi upregulates gene expression of tumor suppressors such as *p21* through histone hyperacetylation,[12–14] HDACi does not always upregulate gene expression but induces malignant cell death by downregulating gene expression such as anti-apoptotic genes. In addition, some HDACi compounds exhibited anti-cancer effects through acetylation of non-histone substrates such as heat-shock protein 90 (HSP90),[15] α-tubulin,[16] p53[17] and nuclear factor-κB.[18] For example, Bali *et al.*[15] reported that HDACi caused leukemia cell death by hyperacetylation of HSP90. Hideshima *et al.*[19] demonstrated that tubacin, a specific HDAC6 inhibitor, was effective in augmenting cell death mediated by bortezomib, a proteasome inhibitor, by inhibiting the protein degradation through blocking aggresome activity. Thus, the cell growth inhibitory action of HDACi could be exhibited at the protein expression level.

Here we demonstrate the therapeutic efficacy of NCH-51 on lymphoid malignant cells. NCH-51 induced cell death, more strongly than SAHA. We analyzed the protein expression profiles and found that NCH-51 modulated the expression of antioxidant molecules at the protein level. NCH-51 sustained the intracellular reactive oxygen species (ROS) greater than SAHA.

Correspondence: Professor T Okamoto, Department of Molecular and Cellular Biology, Nagoya City University Graduate School of Medical Sciences, 1 Kawasumi, Mizuho-cho, Mizuho-ku, Nagoya, Aichi 467-8601, Japan.
E-mail: tokamoto@med.nagoya-cu.ac.jp
Received 22 March 2007; revised 6 June 2007; accepted 11 July 2007

a

Cell type		Cell line name	24h		72h	
			SAHA	NCH-51	SAHA	NCH-51
T-cell	T-ALL	Jurkat	0.90	0.92	0.63	0.75
	ATL	MT-2	>30.00	7.81	0.54	2.08
		ATL-102	>30.00	5.80	3.70	2.25
		ED-40515 (-)	1.45	0.94	0.90	0.76
B-cell	CLL	MEC2	>30.00	0.71	0.70	0.47
		MO1043	>30.00	7.67	0.76	0.79
	BL	Raji	>30.00	1.65	0.84	0.71
		Daudi	>30.00	>30.00	>30.00	11.74
	MM	U266	7.67	1.36	0.53	0.66
		XG7	>30.00	2.00	0.73	1.11
		KMS	>30.00	>30.00	1.35	3.43
		ILKM-2	1.41	1.11	0.61	0.66
		RPMI8226	5.72	2.82	2.92	2.72

Growth inhibition (%)

80-100
60-80
40-60
20-40
0-20

Each Value means IC_{50}

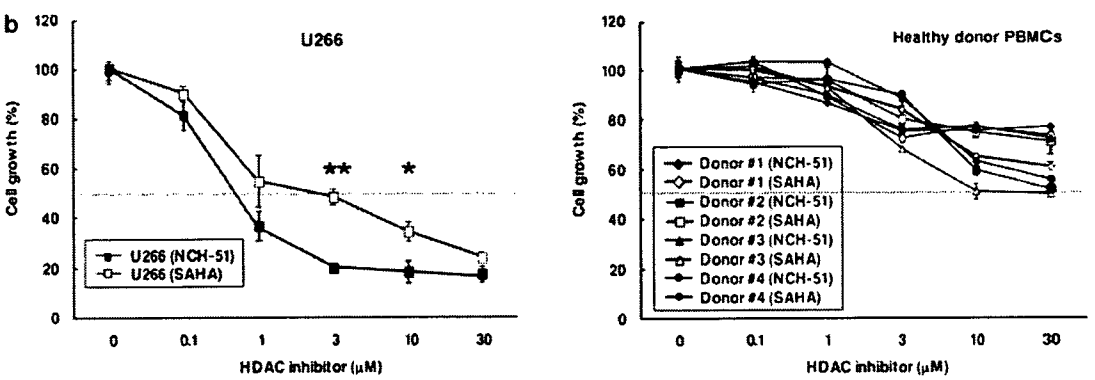

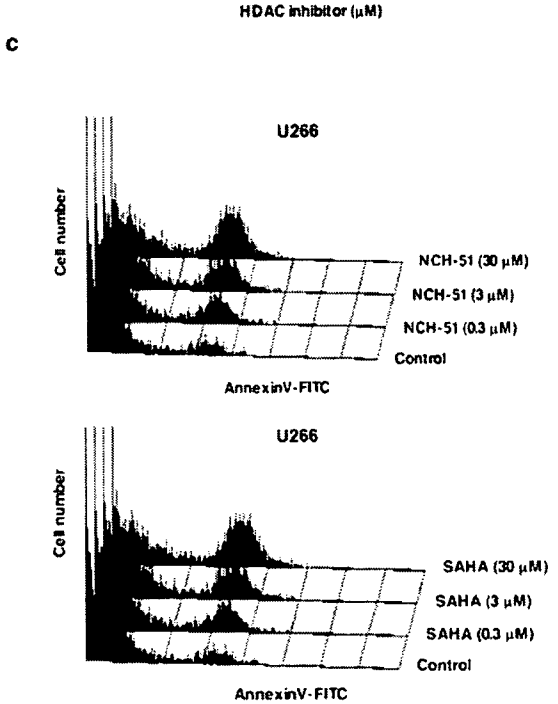

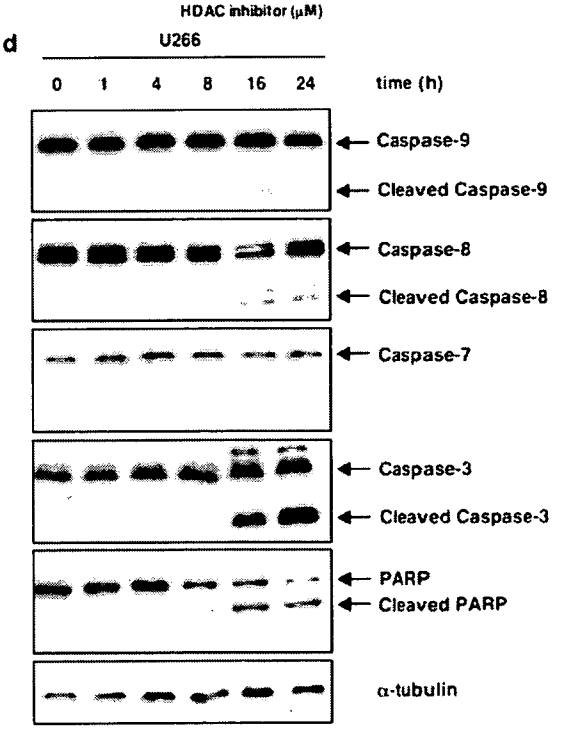

Materials and methods

Cell lines and reagents

A human acute T-cell leukemia cell line, Jurkat, ATL cell lines, MT-2, ATL-102 and ED-40515(−), chronic lymphocytic leukemia cell lines, MEC2 and MO1043, Burkitt's lymphoma cell lines, Raji and Daudi and multiple myeloma cell lines, U266, XG7, KM5, ILKM-2 and RPMI-8226 were used in this study as described previously.[20–24] For normal controls, peripheral blood mononuclear cells (PBMCs) were obtained from four independent healthy donors upon informed consent after the approval of Institutional Ethical Committee. All cells were cultured in RPMI-1640 medium, supplemented with 10% fetal bovine serum at 37°C in a 5% CO_2 incubator. NCH-51, a novel non-hydroxamate HDACi, and SAHA, a conventional hydroxamate HDACi, were synthesized by us as described previously.[11] NCH-51 and SAHA were dissolved in dimethyl sulfoxide at 50 mM and stored at −20°C. An antioxidant compound *N*-acetyl-L-cysteine (NAC) was purchased from Sigma (St Louis, MS, USA).

Growth inhibition assay

Growth inhibitory effect of HDACi was determined using 3-(4,5-dimethylthiazol-2-yl)-2,5-diphenyltetrazolium bromide assay (Sigma) as described previously.[25] Briefly, approximately $1–10 \times 10^4$ cells per 100 μl were cultured in 96-well plate in triplicates at 37°C. Optical densities (OD) at 570 and 630 nm were measured with a multiplate reader. Cell growth (%) was calculated as follows: (OD_{630}–OD_{570} of the samples/OD_{630}–OD_{570} of the control) × 100.

Apoptosis and cell cycle analysis

Apoptosis and cell cycle analyses were performed as described previously.[20] For apoptosis analysis, the cells were treated with or without HDACi for 18 h, and incubated with fluorescein isothiocyanate (FITC)-conjugated annexin V (MBL, Nagoya, Japan). The cell numbers of annexin V-positive cells were analyzed by flowcytometry (FACScan, BD Bioscience, San Jose, CA, USA) and CellQuest analysis program (BD Bioscience). For cell cycle analysis, the cells were incubated with or without HDACi for 24 h, washed with cold phosphate-buffered saline (PBS), and fixed with 70% ethanol. After incubation with RNase A (Qiagen, Alameda, CA, USA), the cell pellets were resuspended in PBS containing propidium iodide (Sigma). DNA content of each cell preparation was analyzed by flowcytometry.

Protein extraction for proteome analysis

Proteome analysis was performed according to Seike *et al.*[26] U266 cells were incubated with or without 3 μM NCH-51 for 18 h. The cell pellets were washed with cold PBS and then treated with 10%trichloroacetic acid for 30 min on ice. After washing with PBS, the pellets were collected and resuspended in lysis buffer (30 mM Tris–HCl (pH, 8.5), 7 M urea, 2 M thiourea, 3% 3-((3-chlamidopropyl) dimethylammonio)-1-propanesulfonic acid and 1% Triton X-100). Samples were then subjected to a Dounce homogenizer for 30 strokes and sonicated for 5 min in a sonicator (UCW-201, Cosmobio Co. Ltd., Tokyo, Japan). After incubation for 30 min, the samples were centrifuged at 10 000 × *g* for 30 min followed by ultracentrifugation at 100 000 × *g* for 1 h, and the supernatants were collected. Protein concentration was determined by 2D-Quant kit (GE Healthcare Bio-Sciences Corp., Piscataway, NJ, USA). Fifty micrograms of each protein extract, adjusted to pH 8.5, were labeled with 200 pmol of minimal dye CyDye (GE Healthcare Bio-Sciences Corp.). NCH-51-treated samples and untreated control proteins were labeled with Cy3 and Cy5, respectively. Internal control, consisting of half part of each paired sample was labeled with Cy2. Labeling reaction was stopped with the addition of 0.2 mM L-lysine (Sigma) for 10 min on ice. Each labeled sample was mixed into one tube and then incubated with an equal amount of lysis buffer for 10 min on ice. The final volume was adjusted to 450 μl with DeStreak Rehydration Solution and 0.5% IPG buffer (GE Healthcare Bio-Sciences Corp.).

Two-dimensional (2D) electrophoresis and image analysis

An immobilized pH gradient gel Immobiline DryStrip (GE Healthcare Bio-Sciences Corp.), with non-linear pH values (3–10), was rehydrated with the labeled protein samples at 20°C for 12 h. Isoelectric focusing was performed using IPGphor (GE Healthcare Bio-Sciences Corp.) at 20°C for total 65 000 khT. Immobiline DryStrips were then equilibrated for 15 min in the buffer (6 M urea, 1.5 M Tris–HCl (pH 8.8), 30% glycerol, 2% sodium dodecyl sulfate) containing 10 mg/ml dithiothreitol and prolonged for 15 min in the same buffer containing 25 mg/ml iodoacetamide. After equilibration, Immobiline DryStrips were transferred onto 11.5% polyacrylamide gels and run in the EttanDalt Six system (GE Healthcare Bio-Sciences Corp.) at 30 W/gel for 5 h at 20°C. The gels were scanned with appropriate wavelengths for excitation and emission using Ettan DIGE Primo (GE Healthcare Bio-Sciences Corp.). Relative quantification of spot intensities and statistical evaluation were carried out with ImageMaster 2D Platinum software (GE Healthcare Bio-Sciences Corp.). The experiments were performed in quadruplicates. The protein spots that were statisti-

Figure 1 Induction of apoptosis by a novel HDAC inhibitor NCH-51. (**a**) The growth inhibitory effects of NCH-51 and suberoylanilide hydroxamic acid (SAHA) on 13 lymphoid malignant cell lines. The cells were treated with either NCH-51 or SAHA (3 μM) for 24 or 72 h. Cell growth was estimated by 3-(4,5-dimethylthiazol-2-yl)-2,5-diphenyltetrazolium bromide (MTT) assay and gray-scale levels represent the growth inhibition rate (%) compared to untreated control. Each value indicates the mean IC_{50}. (**b**) Growth inhibitory effects of NCH-51 and SAHA on U266 cells and four control peripheral blood mononuclear cells (PBMCs). A multiple myeloma cell line U266 cells, and four healthy donor PBMCs were treated with indicated concentrations (0–30 μM) of NCH-51 (closed symbols) or SAHA (opened symbols) for 24 h. Cell growth was evaluated by MTT assay. The results are shown as the percentage cell growth compared to untreated control. These experiments were performed in triplicates and the mean values ± s.d. are shown. $^*P<0.05$; $^{**}P<0.01$. (**c**) Induction of apoptosis by NCH-51. U266 cells were treated with the indicated concentrations (0–30 μM) of NCH-51 for 18 h, stained with fluorescein isothiocyanate-conjugated annexin V, and analyzed by flowcytometry. Annexin V-positive fraction indicates the cells undergoing apoptosis. (**d**) Activation of caspases and poly-ADP ribose polymerase (PARP) cleavage by NCH-51. U266 cells were treated with 3 μM of NCH-51 for 0–24 h. Whole cell extracts were prepared and subjected to immunoblots with the indicated antibodies. Positions of uncleaved (inactivated) and cleaved (activated) caspases and PARP proteins are indicated by arrows.

cally significant between untreated control and treated sample were selected.

Protein identification by mass spectrometry

For mass spectrometric analysis, 400 μg of unlabeled-protein extract was independently applied to 2D electrophoresis. The gel was stained with DeepPurple solution (GE Healthcare Bio-Sciences Corp.) according to the manufacturer's recommendation. The gel image was obtained by scanning with Ettan DIGE Primo and matched to those of analytical gels by using the ImageMaster 2D Platinum software. The spots of interest were picked out, and in-gel protein digestion was carried out with trypsin gold (Promega, Madison, WI, USA) as described.[26] Mass spectrometric analyses were performed by using a MALDI-TOF/TOF type mass spectrometer AB4700 (Applied Biosystems, Framingham, MA, USA). The proteins were identified through the online search using MASCOT database search engine.

Immunoblot analysis

The cell extracts obtained from cell cultures treated with or without HDACi were subjected to cell extract preparation as described above. The samples were applied to electrophoresis on a 10% polyacrylamide gel and transferred onto a nitrocellulose membrane. The membranes were incubated in TBS-T (10 mM Tris–HCl (pH, 8.0), 150 mM NaCl, 0.1% Tween) with 5% non-fat milk containing 1:1000 diluted primary antibodies against either caspase-9, -8, -7, -3, poly-ADP ribose polymerase (PARP) (Cell Signaling Technology, Danvers, MA, USA), peroxiredoxin 1 (Affinity Bioreagents, Golden, CO, USA), elongation factor-2 or α-tubulin (Santa Cruz, Santa Cruz, CA, USA). Membranes were then rinsed in TBS-T and further incubated with HRP-conjugated secondary antibody (GE Healthcare Bio-Sciences Corp.) in TBS-T with 5% non-fat milk. Each protein was detected by SuperSignal (PIERCE, Rockford, IL, USA).

Detection of ROS

ROS content was measured as described previously.[27] After treatment with HDACi, the cells were incubated with an oxidation-sensitive fluorescent probe 2′, 7′-dichlorofluorescein diacetate (H_2-DCFDA) (Molecular Probes Inc., Eugene, OR, USA) at a final concentration of 5 μM for 30 min. The cells were washed and resuspended in PBS, and then ROS amount was measured by flowcytometry.

Results

NCH-51 induces apoptosis greater than SAHA

We first evaluated the growth inhibitory effects of NCH-51 on a variety of lymphoid malignant cell lines (Figure 1a). A tentative result in a multiple myeloma cell line U266 cells is shown in Figure 1b. In most of the cell lines including U266 cells, NCH-51 exhibited a stronger growth inhibitory effect than SAHA at 3 μM for 24 h treatment, whereas prolonged incubation for 72 h did not show such a difference. It is noted that there was no significance in the growth inhibitory effect on four healthy donor PBMCs between NCH-51 and SAHA (IC_{50} values of both agents were higher than 30 μM), suggesting a cell-type specific cytotoxicity of NCH-51. We then analyzed the apoptosis and cell cycle distribution after the treatment with NCH-51 or SAHA. In the six cell lines (Jurkat, ED-40515(−), MEC2, U266, XG7 and ILKM-2), all of which showed a high susceptibility to NCH-51 ($IC_{50}<3$ μM), NCH-51 strongly induced apoptosis greater than SAHA after 24 h treatment as demonstrated by generation of sub-G_1 cells (Figure 1c and Table 1). In fact, when U266 cells were treated with NCH-51, cleaved forms of caspase-9, -8, -3 and PARP could be detected after 8 h, evidently at 16 h, although no activation of caspase-7 was detected (Figure 1d), suggesting that NCH-51 induces apoptosis through both extrinsic (type I) and intrinsic (type II) pathways[28] in the short-term treatment. On the other hand, cell cycle analysis revealed that NCH-51 increased the cell number at G_2/M-phase and reduced the number at G_1- or S-phase in most of the cell lines examined (Table 1, right column). No significant difference in the effects on cell cycle regulation was observed between NCH-51- and SAHA-treated cells. These observations suggest that the apoptosis-inducing activity might be attributable to the difference in the observed growth inhibitory effects between NCH-51 and SAHA.

NCH-51 regulates the expressions of antioxidant molecules at the protein level

To identify the target molecules regulated by NCH-51, we analyzed the RNA and protein expression profiles. cDNA microarray analysis using U266 cells showed that NCH-51 treatment upregulated the expression of *p21* and *p19* (Supplementary Table 1), confirming the previous reports by us[11] and others.[12–14] On the other hand, NCH-51 downregulated the gene expression of *CFLAR* (*c-FLIP*), *survivin* and *BCL2L2* (*bcl-w*), which act as antiapoptotic molecules. These results suggested that these genes were responsible for the growth inhibitory action of NCH-51, however, there was no notable difference in mRNA expression between NCH-51- and SAHA-treated cells. We then performed the proteome analysis. Whole cell extracts were prepared from U266 cells treated with or without NCH-51, and the protein samples were labeled with fluorescent dyes and applied to 2D electrophoresis (Figure 2a). By comparing the amounts of cellular proteins, we identified 14 proteins that varied relatively to NCH-51 treatment (Table 2). Ten proteins including nucleotide diphosphate kinase A (NDPKA), peroxiredoxin 1 and 2 (PRDX1, 2), glutathione *S*-transferase P1-1 (GSTP1-1), 14-3-3 zeta/delta, Cl^- intracellular channel proteins 1 and 4 (CLIC1, 4), proteasome subunit α3, protease activator 28 β subunit and Rho GDI α were upregulated, and four proteins including alanyl-tRNA synthetase (AARS), elongation factor-2 (EF-2), heat-shock 70 kDa protein 8 (HSPA8) and mitochondrial inner membrane protein, were downregulated after the treatment with NCH-51. Interestingly, some of these proteins upregulated by NCH-51 belong to a class of antioxidant molecules. It is noted that PRDX1 and PRDX2 were upregulated at both mRNA and protein levels, thus they are considered to be upregulated at the gene expression level, whereas most of the proteins were upregulated without induction at the gene expression level. In contrast, EF-2 and HSPA8 were downregulated at the protein level. The effects of NCH-51 and SAHA on the expression of EF-2 and PRDX1 were then verified. As shown in Figure 2b, EF-2 protein level was decreased either by NCH-51 or SAHA in the cell lines such as U266, ED-40515 (−) and XG7 cells that were highly susceptible to HDACi. EF-2 was decreased after 16 h treatment with these HDACi (data not shown). On the other hand, in the cell lines such as MEC2, Daudi and KM5 cells that were less sensitive to HDACi, EF-2 protein level was not significantly changed. PRDX1 protein level was upregulated by the treatment with either NCH-51 or SAHA in ED-40515 (−), U266, XG7 and MEC2 cells. SAHA seemed to upregulate PRDX1 more than NCH-51.

Table 1 The profiles of apoptosis and cell cycle distribution

Cell line	*HDAC inhibitor (μM)*	*Apoptotic cell[a] (%)*	*Cell cycle distribution[a](%)*			
			sub G_1	*G_1*	*S*	*G_2/M*
Jurkat	Untreated control	6.30	5.11	50.39	20.76	20.64
	SAHA					
	3 μM	13.45	28.56	9.15	12.97	46.22
	30 μM	28.97	32.39	7.06	18.10	40.83
	NCH-51					
	3 μM	19.27	42.66	8.05	10.04	36.28
	30 μM	35.45	42.69	7.64	14.41	32.21
MT-2	Untreated control	6.84	3.02	63.25	15.29	15.64
	SAHA					
	3 μM	8.23	9.41	49.04	11.70	26.36
	30 μM	8.75	10.35	62.95	6.15	13.96
	NCH-51					
	3 μM	8.45	3.26	62.21	16.34	16.53
	30 μM	8.62	5.38	71.64	8.35	12.22
ED-40515 (−)	Untreated control	6.44	8.40	46.82	23.30	19.67
	SAHA					
	3 μM	20.74	18.88	21.41	19.07	36.90
	30 μM	20.12	26.87	22.20	20.49	27.75
	NCH-51					
	3 μM	22.12	27.10	28.04	19.04	23.91
	30 μM	21.33	26.54	25.09	20.56	25.72
MEC2	Untreated control	3.20	5.66	60.06	19.96	12.16
	SAHA					
	3 μM	4.84	12.32	37.33	19.84	26.70
	30 μM	8.22	18.14	29.46	22.63	25.12
	NCH-51					
	3 μM	6.50	16.22	36.43	19.28	24.75
	30 μM	11.08	21.24	30.47	20.93	23.29
MO1043	Untreated control	4.14	0.89	54.88	20.75	17.87
	SAHA					
	3 μM	4.30	3.45	68.83	7.49	15.41
	30 μM	15.96	18.85	48.29	6.62	23.14
	NCH-51					
	3 μM	3.74	2.47	73.90	7.17	12.88
	30 μM	14.93	21.75	48.79	6.14	21.03
Daudi	Untreated control	1.62	1.62	52.02	22.77	19.55
	SAHA					
	3 μM	2.08	2.17	23.65	22.33	46.30
	30 μM	2.12	2.34	22.83	19.75	48.21
	NCH-51					
	3 μM	2.64	1.90	50.38	14.74	27.71
	30 μM	3.04	2.19	25.68	22.19	43.28
U266	Untreated control	6.17	6.30	67.42	10.99	13.02
	SAHA					
	3 μM	17.65	11.91	56.24	10.35	19.72
	30 μM	29.73	17.06	48.70	12.69	19.68
	NCH-51					
	3 μM	22.90	13.39	54.07	11.60	18.62
	30 μM	32.63	18.90	49.15	13.40	18.94
XG7	Untreated control	7.27	7.58	49.21	20.34	23.37
	SAHA					
	3 μM	8.74	8.50	50.40	8.33	28.32
	30 μM	9.43	15.38	34.23	15.10	28.21
	NCH-51					
	3 μM	11.47	10.00	49.32	8.62	28.62
	30 μM	13.13	17.87	35.44	14.67	27.93
KM5	Untreated control	4.24	2.91	42.15	27.85	23.43
	SAHA					
	3 μM	4.30	6.32	31.85	31.44	26.13
	30 μM	15.96	23.37	20.62	26.19	24.68
	NCH-51					
	3 μM	3.74	6.75	38.34	29.96	20.84
	30 μM	18.46	20.33	27.77	23.29	24.31